Wrocław University of Technology

Electronics, Photonics, Microsystems

Sergiusz Patela, Marcin Wielichowski,
Szymon Lis, Konrad Ptasiński

ADVANCED OPTOELECTRONICS

Wrocław 2011

Wrocław University of Technology

Electronics, Photonics, Microsystems

Sergiusz Patela, Marcin Wielichowski,
Szymon Lis, Konrad Ptasiński

ADVANCED OPTOELECTRONICS

Wrocław 2011

Table of Contents

1 Measurements and analysis of propagation parameters of planar waveguides

1.1 Planar waveguide parameters

Contemporary integrated optoelectronics employs optical planar waveguides as connections between active elements. Considering this trend, planar waveguide have become subject to intense research.

Planar waveguide parameters fall into three basic groups. The groups are given below together with names of the most commonly used parameters:

- o optical
    - o attenuation, refractive index, cut-off thickness, modal properties, temperature stability of parameters
- o geometrical
    - o dimensions (thickness), dimension tolerances, surface topology
- o mechanical
    - o stress

1.2 Optical measurement methods

Experimental investigation into planar waveguide parameters requires an effective method of light wave coupling into the waveguide. The problem of coupling laser-emitted (or coming from other light sources) light beam into optical thin films would, for a long time, be an important area of integrated optics investigations and would pose considerable difficulties.

Among the most frequently used methods of light coupling into optical thin films (planar waveguides) are:

- o butt coupling – which is a direct-coupling method,
- o via distributed couplers – here, methods based on optical prism or grating coupler can be mentioned.

1.3 Butt-coupling

The earliest idea of coupling light into planar waveguide relied on directly illuminating the waveguide edge with light beam being coupled. Light beam emitted by laser (or other light source) is focused at waveguide edge as it is illustrated in figure Fig. 1.1. In this way, guided mode / modes of planar structure (planar waveguide) is / are excited.
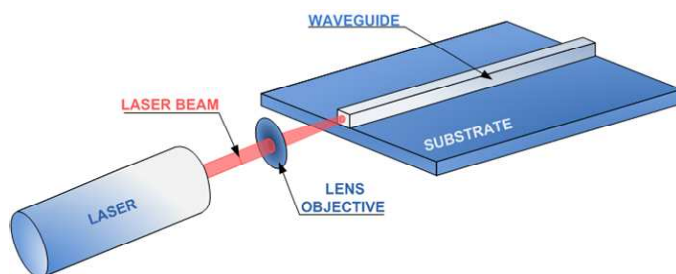
Fig. 1.1 Focused laser beam illuminates waveguide edge thus excites waveguide guided modes – butt-coupling.

Butt-coupling requires high-precision positioning and focusing elements to be used. Light beam should be tightly focused and carefully positioned on waveguide edge. However, due to waveguide edge roughness, excessive light scattering can occur. In the butt-coupling method, different (guided as well as radiation) modes are excited in an uncontrolled manner. Under some circumstances, this may be considered as a disadvantage of the method (Dylewicz, 2007).

1.4 Cut-back method

The butt-coupling method we have just discussed, is part of the so called cut-back method that enables measurements of planar waveguide attenuation. In the cut-back method, optical waveguide (this method can be applied to planar as well as to fiber waveguides) is cut (cleaved) into pieces of different lengths. Before each of the cuts (and after the last cut, of course), light transmission through the remaining part of the waveguide is measured. The cut-back method measurement procedure is illustrated in figure Fig. 1.2.
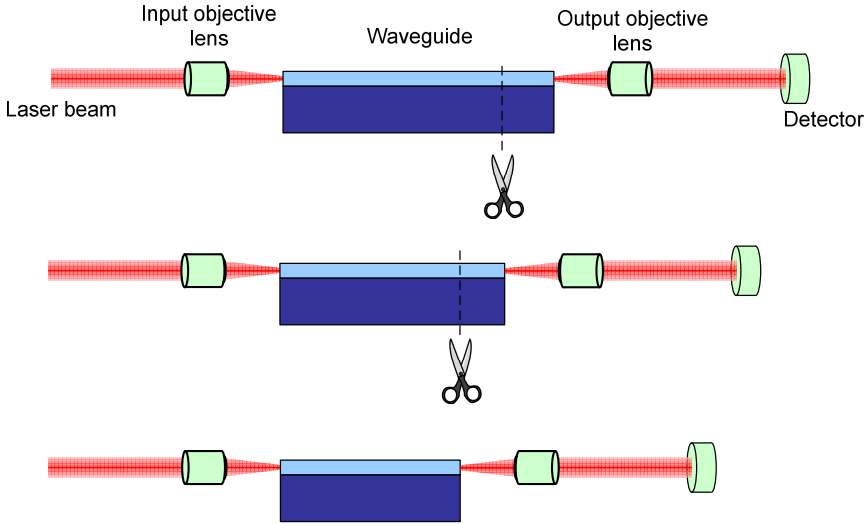
Fig. 1.2 Idea of planar waveguide attenuation measurement by means of cut-back method.

Light transmission can be described with the following formula (Gill, 1996)

$$T(x) = \frac{P_o(x)}{P_i} \cdot \frac{1}{T_{obj.i} T_{obj.o}} \cdot \frac{1}{(1-R_i)(1-R_o)}$$

(1.1)

where: $T_{obj.i}$ and $T_{obj.o}$ are transmission coefficients of objective lenses, R_i and R_o are Fresnel reflection coefficients of waveguide edges (end facets), and P_i and P_o are optical powers. In all cases, the i and o subscripts indicate input and output, respectively. In the cut-method, knowledge of coupling efficiency is unnecessary because there are several values of $T(x)$ measured for different waveguide lengths but each time identical light coupling method is used. Finally, waveguide attenuation can be estimated, and it is usually done so, based on $\log(T(x))$ plotted in the function of waveguide length x.

Cut-back has some potentially significant disadvantages. First of all, it is a destructive method (waveguide needs to be cut). Waveguide edge polishing process that is usually applied after each cut, may also be problematic. Moreover, due to the utilization of the butt-coupling method, simultaneously exited waveguide modes can falsify measurement results (Gill, 1996).

1.5 Prism coupler

The next method of effectively coupling light into planar waveguides is the prism coupler method. This time, light enters the waveguide through its top surface instead of the end surface (end facet) as was the case in butt-coupling. An idea of the prism coupler method (prism coupler principle of operation) is shown in figure Fig. 1.3. A right triangular prism is positioned above the waveguide. A thin air-filled gap is left between the prism and the waveguide. Gap thickness is of the order of half the light wavelength or less. A laser beam enters the prism and then it undergoes total internal reflection at the prism base. Due to the nature of the total internal reflection phenomenon, an evanescent wave is created which penetrates both the air-gap and the waveguide. Provided that a proper relationship between light propagation vectors is maintained (see figure Fig. 1.3 and discussion in paragraph 1.6), part of the evanescent wave's energy turns into guided wave that propagates within waveguide volume (Dylewicz, 2007).
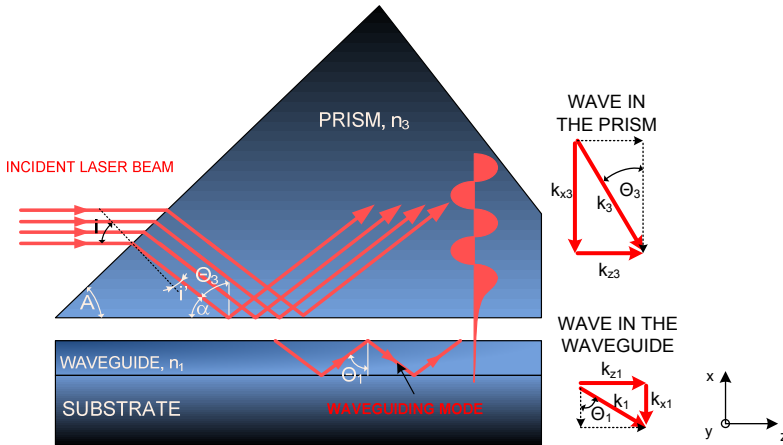
Fig. 1.3 Evanescent wave resulting from total-internal reflection, couples light into planar waveguide – prism coupler.

1.6 General conditions for efficient coupling

There are two fundamental conditions of light coupling by means of a prism coupler. The first conditions can be stated in the following way (Ulrich, 1971):

1. The tangent components of wave velocities in two coupled media must be the same.

In other words, propagation vector component z of lightwave inside the prism (k_{z3}) must be equal to that of lightwave inside the waveguide (k_{z1}). Mathematically, this condition can be expressed as follows

$$k_{z3} = kn_3 \sin\theta_3 = k_{z1} = kn_1 \sin\theta_1 \qquad (1.2)$$

In (1.2), (length of) the propagation vector k is connected with lightwave angular frequency ω, with the relation $k=\omega/c$, where c is the velocity of light in vacuum. Other symbols used in (1.2) are (also compare figure Fig. 1.3): θ_3 is the incident angle of a wave in the prism, n_3 is the refractive index of the prism, θ_1 is the incident angle of wave in the waveguide while n_1 is the refractive index of the waveguiding medium.

The light beam in the prism must have the same phase as a zigzag wave in the waveguide, and this condition should be fulfilled at every point of the planar waveguide. This condition is also know as the synchronous condition.

The second condition of prism coupler-based light coupling is (Ulrich, 1971):

2. The length along the coupled boundary must be adjusted according to the strength of the coupling.

Coupling length depends on a laser beam diameter. Coupling strength is varying as spacing of air gap changes. Coupling efficiencies are reported to be up to 81% (Palais, 1998).

In the prism coupler method, besides the high coupling efficiency that can be achieved, also some disadvantages need to be noted as well:

- o It is fairly difficult to obtain and keep the air gap between the prism and thin-film waveguide constant.
- o The method is sensitive to mechanical vibrations and temperature variations.
- o A high refractive index of the prism is required.
- o It is impossible to attach the prism to an integrated optical circuit of a large or medium scale of integration.

1.7 Effective index evaluation of prism coupler

Based on figure Fig. 1.3, we can calculate (thus also measure) the effective refractive index values of individual guided modes being (selectively) excited by means of a prism coupler. From Snell's law applied to the prism-air interface we have

$$1 \cdot \sin i = n_3 \sin i'$$ (1.3)

Considering an elementary property of triangle angles (angle values sum up to 180°)

$$A + \alpha + (90 + i') = 180$$ (1.4)

Then, by using simple geometrical and trigonometric dependencies, the angle *i'* can be calculated

$$\theta_3 = 90 - \alpha = 90 - [180 - A - (90 + i')] = A + i'$$ (1.5)

$$\sin i' = \frac{\sin i}{n_3}$$ (1.6)

$$i' = \arcsin\left(\frac{\sin i}{n_3}\right)$$ (1.7)

On substituting (1.7) into (1.5), we get the formula for the angle θ_3

$$\theta_3 = A + \arcsin\left(\frac{\sin i}{n_3}\right)$$ (1.8)

Effective refractive index of a guided mode can be written as

$$n_3 \sin \theta_3 = n_1 \sin \theta_1 = N_{eff}$$ (1.9)

After substituting (1.9) into (1.8) we arrive at

$$N_{eff} = n_3 \cdot \sin\left[A + \arcsin\left(\frac{\sin i}{n_3}\right)\right]$$ (1.10)

Formula (1.10) can be interpreted as: effective refractive index values of individual guided modes of a planar waveguide can be determined by measuring only one parameter – angle (*i*) at which light is coupled into the prism.

1.8 Grating coupler
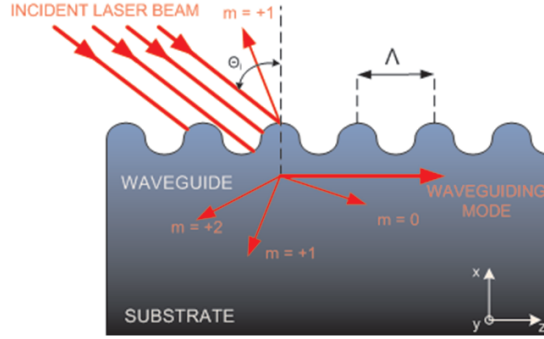
Fig. 1.4 One of diffraction beams can become guided in planar waveguide – grating coupler.

Another method of coupling light into submicrometer optical structures is utilizing a grating coupler. Grating coupler, similarly to prism coupler, couples light into planar waveguide through waveguide's top surface. As it is shown in figure Fig. 1.4, a laser beam impinging on the grating is split into several diffraction beams. One of the beams can become guided provided that it meets certain condition. The condition is: propagation vector component z of one of the diffraction beams is given by (Ogawa, Chang, Sopori, & Rosenbaum, 1973)

$$k_{zd} = k \sin \theta_i + m \left(\frac{2\pi}{\Lambda} \right)$$

(1.11)

where: k is the propagation vector length, θ_i is laser beam angle of incidence, $m = 0, \pm 1, \pm 2,...$ is diffraction order, and Λ is grating period. In other words, grating will serve as a coupler when one of k_{zd} values is equal to one of the values of waveguide mode propagation constant.

The maximum coupling efficiency is reported to be up to 30% (Kogelnik, 1969). A special coupler design with a blazed grating allows efficiencies as high as 97% (T. Aoyagi, Y. Aoyagi, & Namba, 1976).

Grating coupler's advantages over prism coupler are:

- o Flatness of the surface
- o Compactness in size
- o Insensitiveness to temperature variations.

1.9 Effective index evaluation of grating coupler

Analogous considerations (to prism coupling) allow determining effective refractive index for grating coupling (Harper, 2003):

$$N_{eff} = n_1 \sin \theta_m + m \frac{\lambda}{\Lambda}$$

(1.12)

where: n_1 – refractive index of surroundings (frequently $n_1 = n_{air} = 1$), θ_m – coupling angle for the TE/TM optical mode of m-th order, Λ – grating period, λ – light wavelength, m – diffraction order.

1.10 Additional measurement methods

Investigation of planar waveguide optical properties not always involves coupling of light into waveguide structures. There exist a number of measurement methods that, without light coupling into waveguide, enable the determination of key planar waveguide parameters. One of such methods is ellipsometry.

Ellipsometry relies on measuring lightwave polarization changes that are caused by ligtwave reflection off sample surface. In figure Fig. 1.5, an idea of measuring planar waveguides by means of ellipsometry is shown.
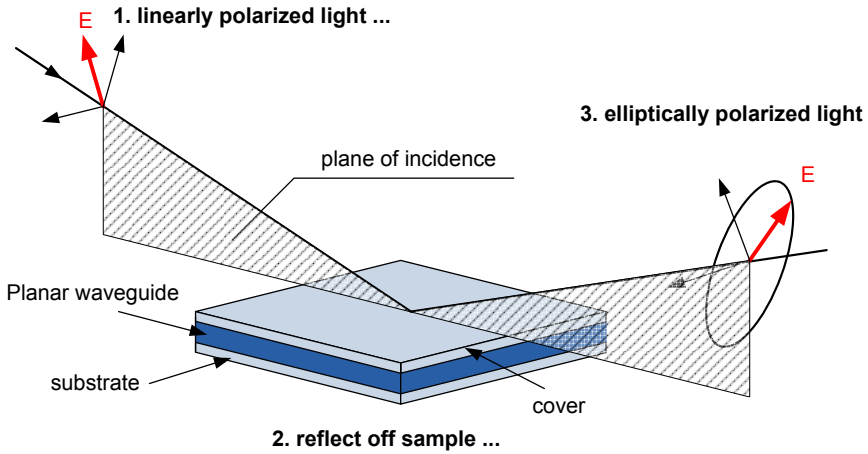
Fig. 1.5 Idea of measuring planar waveguide physical parameters by means of ellipsometry.

Ellipsometry enables the determination (measurement) of the following planar waveguide parameters:

- o refractive index
- o thickness of layers

A detailed description of the method is given in Chapter 5.

Another measurement method, a one that enables measurements of (before all) geometrical parameters of planar waveguides is optical profilometry. Construction details of an optical profilometer are shown in figure Fig. 1.6. In fact, optical profilometer principle of operation is similar to that of interference microscope.
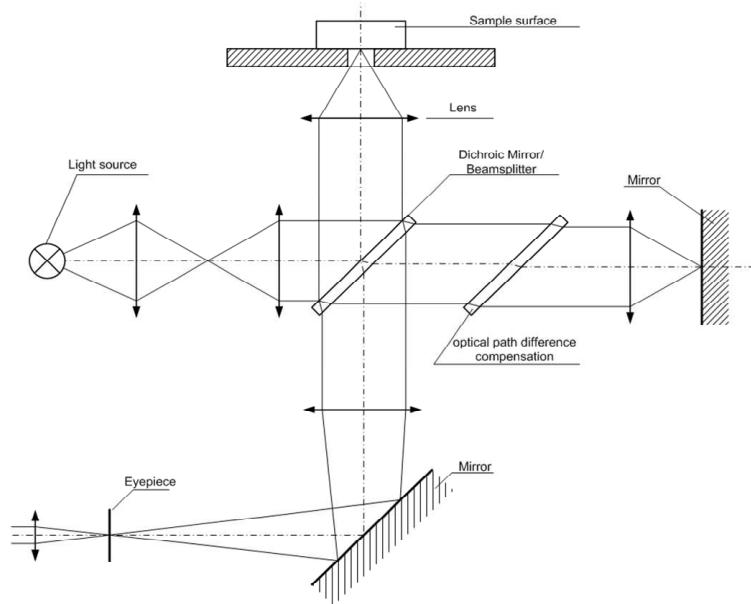
Fig. 1.6 Idea of measuring planar waveguide parameters by means of optical profilometry.

Optical profilometer is a powerful measurement tool. It can easily be adapted to measuring the following planar waveguide parameters:

- o   thickness of layers
- o   stresses in layers
- o   dimensions
- o   surface parameters (e.g. roughness)

In figure Fig. 1.7, details of waveguide surface roughness together with parameters used in their description are displayed.
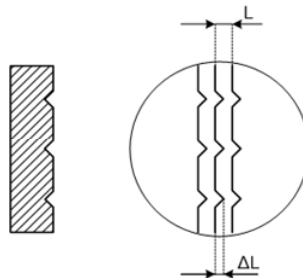
Fig. 1.7 Details of waveguide surface roughness to be measured by means of optical profilometry.

Height of single unevenness is calculated according to the formula

$$R = \frac{\lambda}{2} \frac{\Delta L}{L}$$

(1.13)

Surface roughness is a very important parameter of planar optical waveguides. This is because waveguide surface roughness is a direct source of:

- o transmission losses
- o scattering losses

Optical profilometry is discussed in greater detail in Chapter 5.

2 Fabrication methods of optical layers and planar waveguides

2.1 Overview of photonic technologies

Photonic technologies may be classified into three groups:

- o Optical fiber technology
  Fiber is not only a transmission medium. Other devices such as amplifiers or filters can be also made with fiber. Fiber devices connect well with transmission lines.
- o Microoptic technology
  Devices are made with traditional optical component: microlenses, prisms, filters and diffraction gratings. Assembly is difficult and expensive.
- o Planar waveguide technology
  Devices are fabricated on a surface of a flat piece of material, e.g. semiconductor or dielectric crystal wafer. Devices are made with the technologies of semiconductor chip manufacturing.

All three technologies listed above can be mixed to fabricate advanced photonic devices.

Planar waveguide technology is a preferable technology as far as fabrication of integrated photonic devices is concerned. Photonic devices fabricated with this method are called planar integrated circuits (PIC). The planar integrated circuits offer several advantages over other integrated optoelectronic devices, there are also challenges specific this technology.
Advantages of planar technology

- o For structures containing multitude of interconnected waveguide devices planar technology is simpler, more efficient and cheaper than fiber optic technology. Example: 1x8 f-o splitter.
- o Dimensions can be controlled with greater accuracy than in fiber devices. Examples: Mach-Zehnder modulator, directional coupler.
- o Complex devices, such as e.g. Array Waveguide Grating multiplexers cannot be build with any other technology.
- o Many devices can be made in one process on a single substrate and later cut into separate devices. This greatly reduces fabrication costs.
- o Planar technology is the enabling technology for fabrication of advanced integrated optical devices. Example: Integrated optical spectrum analyzer.

Challenges of planar technology

- o Due to very high precision required, planar devices are very difficult to construct. Dimension control up to 0.25 μm may be required.
- o Photolithographic masks are difficult to fabricate, especially for long and diagonal waveguides
- o Some devices are difficult to fabricate in planar form, e.g. Faraday rotators and optical isolators
- o It is costly and difficult to couple planar devices to optical fibers

2.2 Planar waveguides' fabrication methods

Planar waveguide is a starting structure for fabrication of any advanced photonic integrated circuits. There are several technologies suitable for fabrication of such waveguides. The technologies can be divided into three main groups: heterogeneous, homogeneous and semiconductor technologies. By the heterogeneous technology we understand fabrication

method where the waveguide built of one material is deposited onto a substrate of another material. The homogeneous technology is fabrication of the waveguide inside one bulk of a material. The third group refers to technologies concerned with semiconductor materials. The list of groups with names of respective technologies is given below.

1 .Vacuum evaporation (resistive or by electron gun)
2 .Ion sputtering
3. Deposition from liquid solutions
4. Polymerization in ionic discharge
5. Chemical vapor deposition (CVD)
6. Flame hydrolysis deposition (FHD)

heterogeneous

7. Dopant diffusion
8. Ion exchange
9. Ion implantation

homogeneous

10. Waveguiding by lowering concentration of free carriers
11. Electrooptical waveguides.
12. Epitaxy
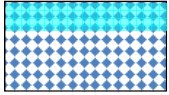
semiconductor

Fig. 2.1Planar waveguide fabrication methods.

The most popular and relatively inexpensive method of thin film deposition used by microelectronic industry is thermal evaporation. The process is conducted under vacuum conditions and enables preparation of layers of any material. However, the structure of the obtained layer is polycrystalline and attenuation of the waveguides is high, well in excess of 1 dB/cm. There exist some modification of the evaporation technology that enables fabrication of waveguides attenuation as low as 0.5 dB/cm, e.g. Ion Assisted Deposition, but they usually introduce complication of technology and additional expenses.

The method of choice, for fabrication of planar heterogeneous waveguides is another vacuum deposition method, namely dielectric film sputtering. Mechanism of deposition and some examples of deposited materials are given on the following figure. On Fig. 2.3 schematic diagrams of deposition systems are given.

target (eg. tantalum)

Ar   Ta

O^{2+}

Ar
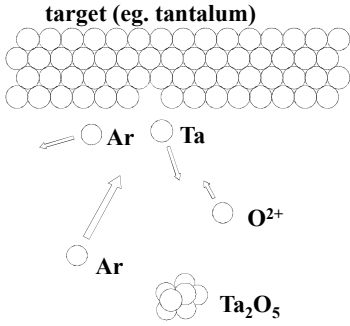
Ta$_2$O$_5$

Examples of waveguide structures prepared by ion sputtering:

Waveguide	substrate
C-7059 glass	KDP
Ta$_2$O$_5$	SiO$_2$(oxidized silicon)
Nb$_2$O$_5$	SiO$_2$(fused quartz)
ZnO	SiO$_2$

Ta$_2$O$_5$, Nb$_2$O$_5$ can be prepared by reactive sputtering from metal targets, or by oxidizing metal layer.

Fig. 2.2 Dielectric films sputtering - principles and materials

d.c.   two-electrode sputtering   r.f..
            systems
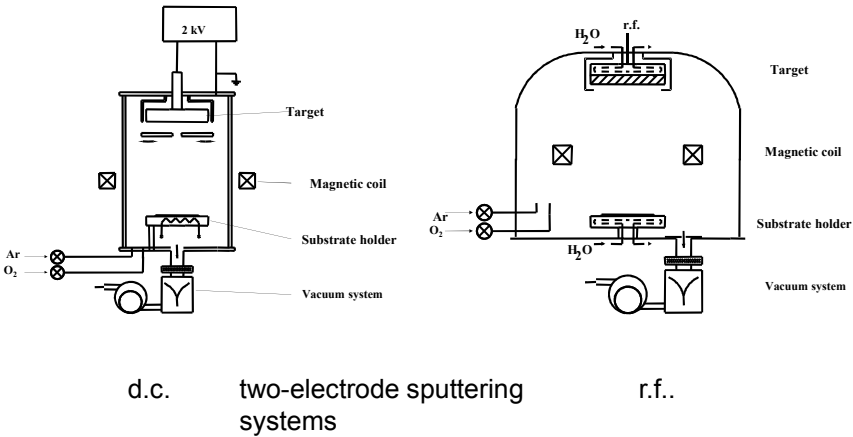
Fig. 2.3 Sputtering of dielectric films – examples of equipment

Dielectric layers obtained with the sputtering methods are characterized by amorphic structure, better surface smoothness and lower attenuation, typically below 1 dB/cm. In the figure below microscopic pictures of surfaces of layers obtained are compared with ion sputtering (left) and evaporation (right).
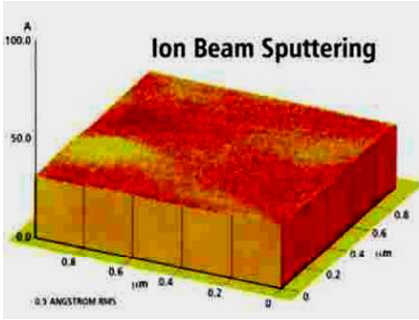
0.05 nm rms roughness   0.4 nm rms roughness
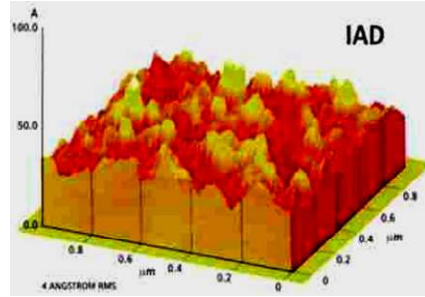
Fig. 2.4 Sputtering versus evaporation - a comparison [Optical Coating by Ion Beam Sputtering, Internet, retrieved 2010 November 14, http://www.oxfordplasma.de/process/opt_coat.htm]

Both evaporation and sputtering methods are "borrowed" from microelectronic and are relatively expensive. An inexpensive alternative is deposition of waveguide layers from liquid solutions. Summary of methods of deposition from liquid solution is given in the following figure.
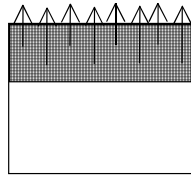
substrate is covered with liquid solution, that after drying leaves solid layer (also sol-gel methods)
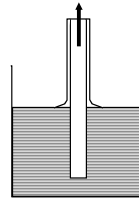
dip-coating: slow and uniform extrusion from solutions (including Langmuir-Blodget method)
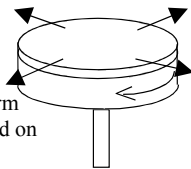
spin-coating: uniform distribution of liquid on a rotating substrate
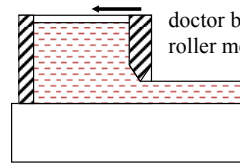
doctor blading (and roller methods)

Fig. 2.5 Methods of deposition from liquid solutions.

The heterogeneous waveguides are characterized by acceptable, but relatively high attenuation. The best heterogeneous waveguides till now were obtained with the method of polarization in ionic discharge.

15
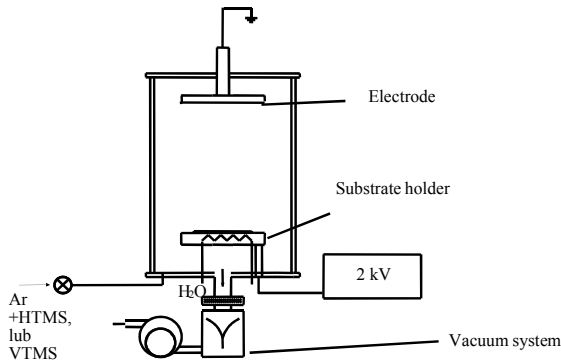
Used chemical compounds:
- vinylo-tri-methyl-silane (VTMS n=1.531), CH2=CH-Si(CH3)3
- heksa-methylo-di-siloxan (HMDS n=1.4704), (CH3)3Si-O-Si(CH3)3
Substrates
- Microscopic substrate glass slides (n=1.512)
-   Corning 744 Pyrex glass (n=1.4704)
Waveguide attenuation 0.03 dB/cm

Fig. 2.6Polymerization in ionic discharge

2.3   Diffusion and ion exchange

Planar waveguides are usually only a starting point for fabrication of more advanced structures. These more advanced structures require additional processing of the layers, for example part of the material is etched to obtain a strip waveguides. In structures based on heterogeneous planar waveguides strong scattering of light may occur at the edges of the strips. This scattering is removed or reduced if heterogeneous structures are replaced with homogenous waveguides fabricated by diffusion, ion exchange or ion implantation.

2.3.1   Diffusion into lithium niobate substrates

Waveguides of the type of Ti:LiNbO3 are obtained by diffusion from metallic layer (Ti) obtained by ion sputtering. Waveguide attenuation 1 dB/cm.

The process is performed at temperature range from 900 to 1150°C, in an atmosphere of argon, nitrogen, oxygen or air with diffusion time from 0.5 till 30h. To keep out-diffusion of LiO from the substrate surface at low level, diffusion is carried out in the atmosphere containing water vapor.

2.3.2   Ion exchange

Ion exchange is a process similar to diffusion, but performed at significantly lower temperatures. Dopant modifying refractive index of the material is exchanged with some ion of the substrate, typically sodium. Schematic illustrating principles of the method is presented below.

16
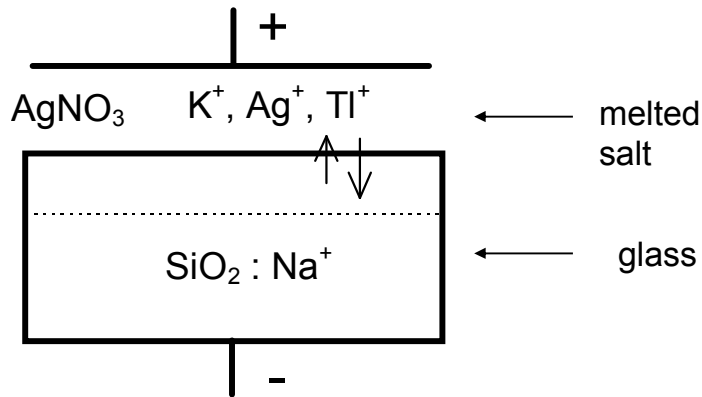
Fig. 2.7 Ion exchange - principle of the effect

Example of the setup used for fabrication of ion-exchange waveguides is presented on the figure below.
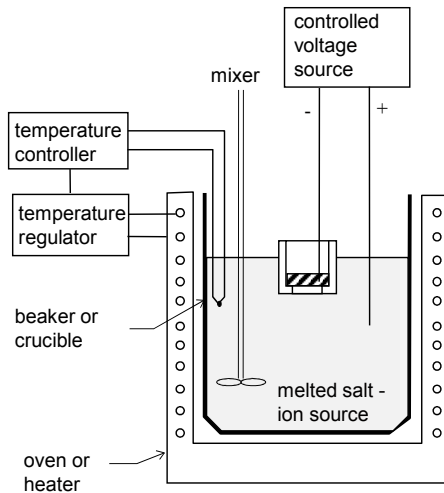
Fig. 2.8 Ion exchange in glass - apparatus

2.4 Fabrication of semiconductor waveguide – epitaxial growth

Basic concept of epitaxial growth is to start with substrate of bulk semiconductor (e.g., GaAs or InP) polished to a flat surface (a wafer), with a particular crystal orientation (e.g., (100) direction). Then grow thin layers epitaxially on the substrate (i.e. with a high-quality crystalline structure based on that of the substrate template). The method enables deposition of thin layers of different materials, with modified alloy compositions and doping.

Three main techniques:
1. Liquid phase epitaxy (LPE)

2. Metal organic vapor phase epitaxy (MO-VPE or MOCVD)
3. Molecular beam epitaxy (MBE)

2.4.1 Liquid phase epitaxy (LPE)

Basic concept of LPE is thermodynamic equilibrium growth. The method may be summarized as follows:

- o Pass a saturated melt of a compound (eg. As in Ga) to be grown over surface of a substrate and reduce the temperature, which reduces the solubility of As and results in deposition of GaAs
- o Horizontal growth technique
- o Substrate is pulled in sequence under several different melts to grow a multiple layer structure
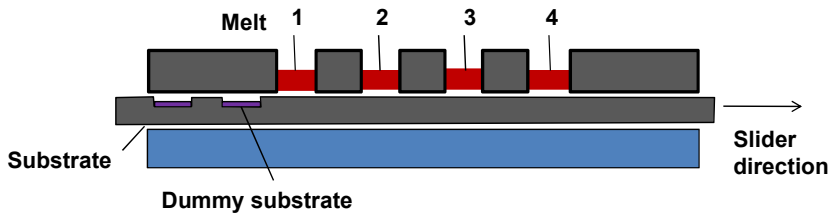
Fig. 2.9 Liquid phase epitaxy (LPE)

Advantages of LPE

- o Thermal equilibrium growth – very low native defect density
- o high radiative efficiency – excellent lasers and LEDs
- o Simple, low cost equipment and high throughput
- o No toxic gases and easily handled solids

Disadvantages of LPE

- o Poor surface/interface morphology
- o Unintentional grading of heterojunctions – both doping and composition
- o Impossible to grow many (20) layer complex heterostructures
- o Difficult to control thickness of thin epitaxial layers
- o Difficult to grow lattice mismatched structures

2.4.2 OM-VPE vapor phase epitaxy

In contemporary photonic OM-VPE is the dominant form of VPE growth of semiconductor heterostructures. Organo-metallic VPE (OM-VPE) is also commonly known as metal-organic chemical vapor deposition (MO-CVD).

18
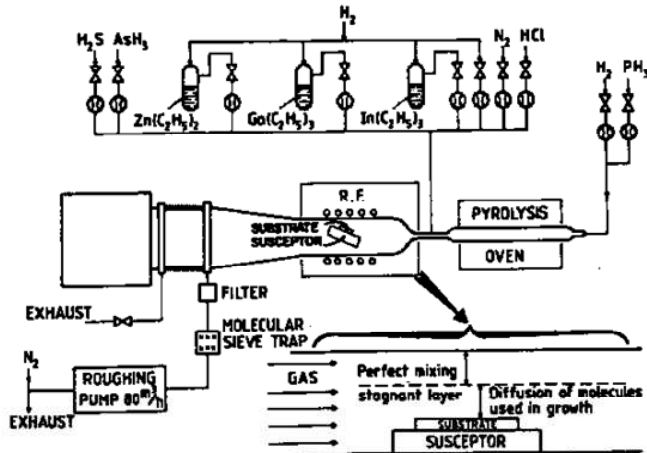
Fig. 2.10Schematic of epitaxial system for OM-VPE vapor phase epitaxy

OM-VPE growth characterization:

- o Materials are transported to substrate using hydrogen gas, at either atmospheric pressure or low pressure of 25-75 torr (1/10 atm)
- o Substrate is heated to 500-700-1000°C (InGaAs-GaAs-GaN)
- o Source materials pyrolyze (thermally decompose) at the substrate surface and material grows epitaxially on the substrate

Advantages

- o Excellent surface and interface morphology and thickness control
- o Precisely controlled abrupt or graded heterojunctions
- o Possible to grow many (100's) layer complex heterostructures
- o Unique possibilities for patterned or localized growth
- o Easier to grow some mixed column V alloys (AsPorAsSb), but much harder to grow mixed nitrides (NAs, NP, NAsSb)
- o Potentially easier large area, multiple wafer scale-up

Disadvantages

- o Safety concerns - large quantities of serious toxic gases (AsH3)
- o Problems with starting material purity
- o Large area doping and compositional uniformity problems
- o Moderately long transients for composition or doping changes
- o Some memory effects

2.4.3 Molecular beam epitaxy MBE

Short summary of the process of MBE:

- o Hot ovens (effusion or Knudsen cells) contain elements to be grown
- o Placed in an extremely high vacuum (e.g., <10-10 torr)
- o Beams of atoms or molecules of the elements evaporate from the ovens
- o Pressure so low that these remain as beams – no chemical reactions before the atoms reach the substrate
- o Atoms reach the heated substrate, react and materials grow epitaxially
- o Substrate rotation is important to improve the growth uniformity
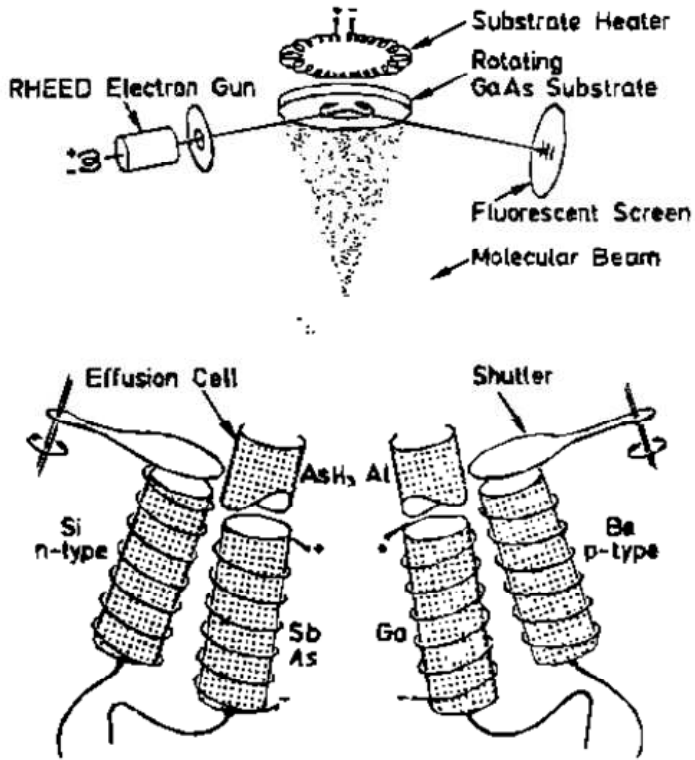
Fig. 2.11 Schematic diagram of MBE growth system

Advantages:

- o Excellent surface/interface morphology and thickness control
- o Precisely controlled abrupt heterojunctions
- o Possible to grow many (100's) layer complex heterostructures
- o In-situ characterization tools (RHEED, Mass Spect., Reflectivity)
- o Easier to grow mixed column III alloys (GaInAl) and dilute nitrides (NAs, NP, NAsSb)
- o High purity elemental starting materials readily available
- o No toxic gases, easily handled solids
- o Relatively simple chemistry

Disadvantages and difficulties:

- o Complex graded interfaces difficult
- o Structures with many different compositions (only 4 metal sources in most machines--now overcome in vertical production machines)
- o Flux transients
- o Run-to-run reproducibility of layer thickness and composition
- o Surface "oval defects"
- o Nucleation of GaNorAlN on sapphire

2.5 Fabrication of strip waveguides and other structures

Following the deposition of waveguiding layer is the process of imposing some photonic structure onto the waveguides. The pictures below illustrate the process of preparation of

electro-optic modulator based on strip waveguide fabricated in LiNbO$_3$ substrate. The first picture illustrates fabrication of the waveguide itself, the second shows deposition of electrodes needed for electro-optic light modulation.
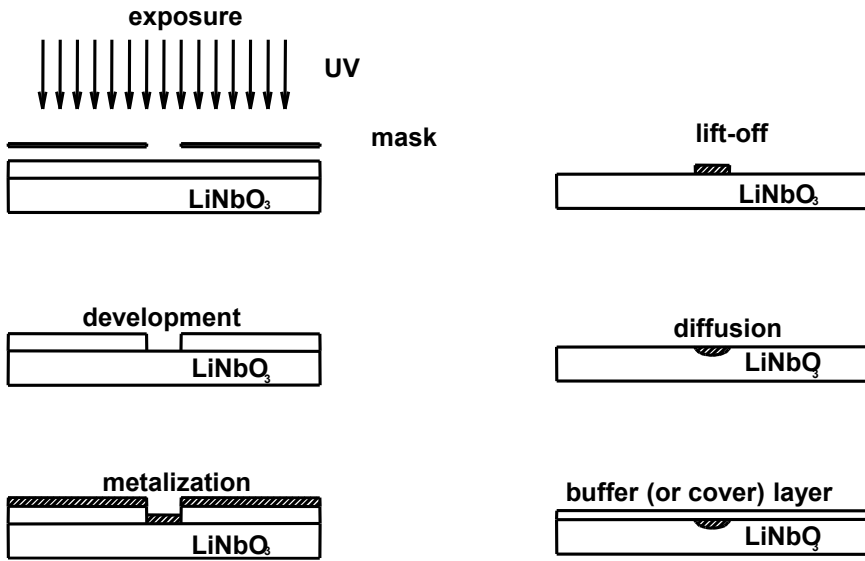
Fig. 2.12 Fabrication of strip waveguides and other structures
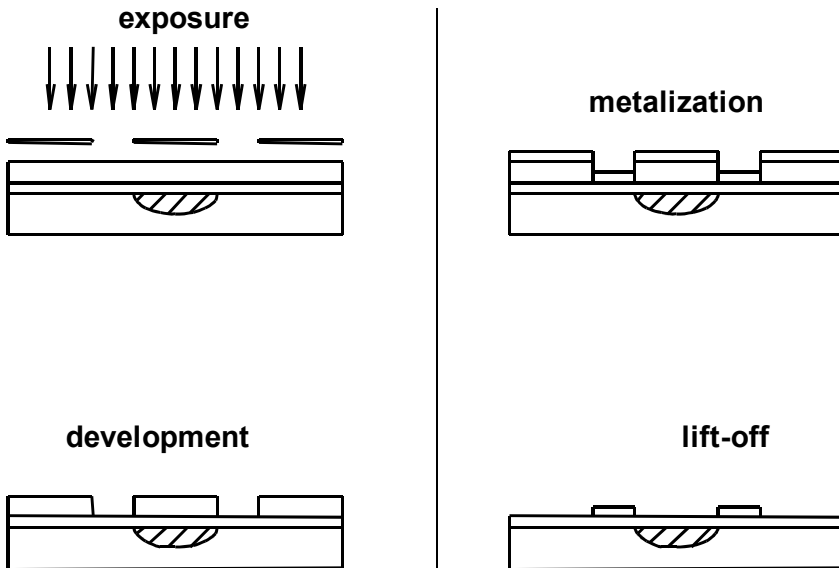
Fig. 2.13Fabrication of waveguide structures - electrodes

3 Waveguides switches and modulators and other devices of integrated optics

3.1 Modulator of light – definition

In telecommunications, the term modulator (not necessarily an optical one) is a device that imposes signal (signal wave, signal train of pulses) on a carrier (carrier wave).

In somehow more general terms, modulation is a process in which changes in one wave train are caused by another wave. Amplitude or frequency modulation in radio transmission are good examples.

In contemporary fiber optics, modulation usually means transferring information from electrical to optical domain – pulses of electric voltage or electric current are transformed into variations in optical power or optical phase or variations in both simultaneously. In subsequent paragraphs we will be studying the techniques of how such modulation can be realized in practice.

To avoid possible ambiguity, let us note that the term modulation is also used with a different meaning in optics. Modulation is regarded there (although this subject will not be discussed in this lecture) as a synonym for contrast, particularly when applied to a series of parallel lines and spaces imaged by a lens (e.g. Spatial Light Modulators).

3.2 Light modulators in photonics

When considering modulators / modulation techniques in photonics, on a general level, we see that they fall into two categories:

1. Direct modulation of a light source – e.g. modulation of electric current flowing through laser diode.
2. External modulators – usually used with CW (continuous-wave) light sources, i.e. light sources the direct modulation of which is difficult due to their physical nature / construction (e.g. gas lasers).

The advantages of external modulation over direct modulation, which are relevant to telecommunications, are discussed in the next paragraph.

3.3 Why do we need external light modulators?

External light modulators allow achieving several goals, which might be difficult or even impossible with direct modulation. Advantages of external modulators are the more pronounced, the higher the modulation frequency is. In fact, high (on the gigahertz level) modulation frequencies are often required in contemporary telecommunications. External light modulators are then needed because of the following reasons:

- for some light sources direct modulation is impossible (e.g. fiber lasers),
- semiconductor light sources chirp (change wavelength) when modulated,
- modulation speed is limited by the electrical capacitance of the source and the speed of migration of the charge carriers.

As concerns the third of the reasons from the list above, using an external light modulator does not automatically guarantee that e.g. the speed-limiting electrical capacitance of the modulator will be lower than that of the light source. However, when properly designed, external modulators generally allow higher modulation frequencies than light sources under direct modulation. Together with the chirp issues experienced when direct modulation is used (see the second reason in the list), external modulators tend to be the best, and sometimes the only possible choice at telecommunications-level modulation frequencies.

3.4 Parameters of electromagnetic wave

Light modulators modify parameters of the electromagnetic wave. Let's look at the wave equation (3.1) and its solution (3.2) to find, which parameters can be changed (Liu, 2005), (Ziętek, 2005).

$$\nabla^2 \vec{E} - \mu\varepsilon \frac{\partial^2 \vec{E}}{\partial t^2} = 0 \qquad\qquad (3.1)$$

$$\vec{E} = E_0(x, y, z)\exp\left[i\left(\omega t - \beta z\right)\right] \qquad\qquad (3.2)$$

From the above equations one gets a list of parameters that can be manipulated by an optical modulator:

- E_0 - amplitude (intensity),
- Φ- phase,
- P–polarization,
- $\lambda(\omega)$ - wavelength (or frequency)

3.5 Classification of effects utilized in waveguide modulators

To achieve the final functionality of (external) modulator – the modulation of lightwave parameter – it is first of all required to decide which physical effect will be employed to modify the wave. The three following physical effect categories (types) are of most significance in the construction of micro-optical waveguide modulators:

1. Absorptive effects – modifications of modulator material's absorption coefficient lead to light beam intensity changes.
2. Refractive effects – modifications of modulator material's refractive index result in changes of phase or direction of light beam, or change of critical angle in total internal reflection.
3. (Micro)mechanical modulation – modifications in modulator element's geometry (shape) or position lead to changes of light beam propagation direction.

In the paragraph that follows, a number of examples for each of the physical effects, are mentioned.

3.6 The physical effects of light modulation

The list of physical effect types is extended below with a number of exemplary physical effects. The effect names are given as they customarily appear in literature. Most of the names describe the respective effect's physical nature (e.g. optical properties of material are affected by temperature in the thermo-optic effect). Nevertheless, some of the names come form their discoverers (e.g. the Franz-Keldysh effect) and do not give any idea of the effect's physical nature. More in-depth descriptions of individual effects are, however, out of scope of this lecture and thus will not be discussed here.

1. Absorptive effects

    a. Franz-Keldysh effect
    b. Quantum Confined Stark Effect
    c. band filling with free carriers
    d. stimulated emission

2. Refractive effects

    a. electro-optic,
    b. magneto-optic,
    c. elasto-optic
    d. acousto-optic,
    e. thermo-optic
    f. free carriers depletion
    g. polarization control in liquid crystals
    h. all absorptive effects through Kronig-Kramers relations

3. (Micro)mechanical modulation

a. simple mechanical choppers

b. optical scanners

c. MEMS (micro-electro-mechanical systems), MOEMS

3.7 Four types of light modulators

Modulators are named after the effect employed for their operation. The list of most popular modulators in use today is given below.

- Electrooptic and magnetooptic modulators. Materials change refractive index under electric or magnetic fields. Special devices (e.g. a Mach-Zehnder interferometer) required to convert phase modulation into amplitude modulation
- Electro-absorptive modulators. Material or structure changes absorption under applied electric field (e.g. reverse biased p-n junction). EA modulators are usually integrated with LDs.
- Acoustooptic modulators. High frequency sound traveling inside material or structure diffracts light.
- MOEMS modulators. Micromechanical beam deflectors or shutters change light intensity.

3.8 Advantages and applications of optical modulators

The simplest way to modulate a light-wave in optical communication system, is by changing the current driving a laser diode. This is so called "direct modulation". However, in some cases it is necessary to use external modulation instead. The list of advantages of using the external modulators as compared to direct modulation is given below.

Advantages of waveguide modulators:

- increase modulation speed and transmission bandwidth,
- improve modulation quality (lower dispersion and distortion, eliminate chirp and crosstalk)
- make optoelectronic converters obsolete

Applications that require external modulation:

- Telecommunications: multimedia transmission (voice, video, data), ISDN (Integrated Services Digital Network), B-ISDN (Broad band ISDN)
- Aerial terminals
- Fiber optic gyroscopes
- Laser pulse forming

3.9 Laser chirp

Let us consider the following scenario concerning a laser diode driven by pulses of electrical current:

- every time a laser diode emits a pulse of light, free carrier concentration in active area is changed,
- which results in refraction index change,
- which changes wavelength of emitted light.

The change in laser emission wavelength during a single pulse is called laser chirp (laser wavelength chirp). Although absolute values of both the refraction index and wavelength changes are relatively small, they become significant in high-speed optical transmissions. Precisely, the wavelength change, laser chirp, is of direct significance. This is because laser chirp results in spectral widening of laser-emitted light linewidth, which then leads to bigger impact fiber dispersion has on light pulse propagating in fiber. In fast optical telecommunications transmission systems (>10 Gb/s, > 100 km inter-repeater distance) chirp-free modulation is necessary.

One noteworthy exception is predistortion – an intentionally introduced, precisely controlled amount of chirp that cancels dispersion.

3.10 Electro-optical effect: change of phase

Refractive light modulators modify phase of optical wave through manipulation of refractive index of a material.

By definition phase of a wave is the term under exponent in the solution of the wave equation (3.3):

$$\vec{E} = E_0(x, y, z) \exp[i(\omega t - \beta z)]$$ (3.3)

For our analysis we can neglect the term ωt, and if definition of propagation is taken into accoun, constant β phase may be written as:

$$\phi = \frac{2 \cdot \pi}{\lambda} n \cdot L$$ (3.4)

where L is length of modulator active area.

For electrooptic effect, approximate equation describing dependence of refractive index n of material on external electrical field E takes the form:

$$n = n_0 - \frac{1}{2} n_0^3 \cdot \bar{\bar{r}} \cdot E$$ (3.5)

The final form of equation (3.4) depends on the modulator material and design, crystallographic orientation of the material and direction of the applied electrical field.

For GaAs modulator (100) when electric field is applied in <011> direction :

$$\phi_{\langle 01\bar{1}\rangle} = \frac{2\pi L}{\lambda d} n^3 r_{41} V \Gamma$$ (3.6)

V – voltage, Γ - overlap integral, d - inter-electrode distance

For other materials and different modulator design the form of the equation (3.6) is usually different.

3.11 Modulators – basic structures. Solid state

Figure Fig. 3.1 gives a review of typical constructions of electro-optical light modulators. The constructions visible in the figure are based on three different principles of operation, three different physical phenomena are employed. In the cases considered, all phenomena are induced with electrical current or electrical voltage applied to electrodes incorporated in modulator structure. The principles of operation are:

- o modification of material absorption directly resulting in optical power change at modulator output
  - o electroabsorption modulator
- o modification of material refractive index resulting in lightwave phase change at modulator output ...
  - o phase modulator
- o ... or at some point (area) within the modulator leading to destructive / constructive interference of light thus to optical power change at modulator output(-s)

- o Mach-Zehnder modulator
- o directional coupler
- o X coupler
- o mode transformer

- o bending the light beam on a diffraction grating dynamically induced in modulator's volume

  - o acousto-optic modulator (grating is induced by an acoustic wave propagating in modulator)
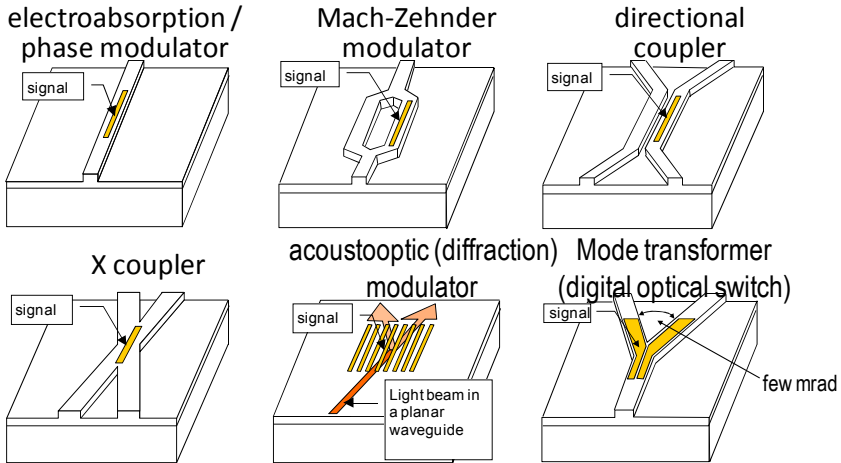
Fig. 3.1 Electro-optical modulators employing absorption, refractive, and diffraction effects.

3.12 Modulators - basic structures. Micromechanical

An idea of another class of light modulators is shown in figure Fig. 3.2. Modulation of light beam is attained by means of mechanically changing the modulator (geometrical) configuration. Principle of operation employed here is

- o modification of light beam propagation path directly resulting in optical power change at modulator output
- o micromechanical light modulator (microoptical waveguide is shifted by a micromechanical actuator)
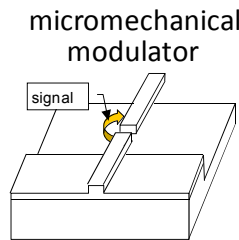
Fig. 3.2 Idea of micromechanical light modulator. Light propagation path is directly changed by micromechanically induced changes in modulator geometry.

Several micromechanical modulators are discussed in greater detail later in this chapter.

3.13 Optical switch (photonic switch) - definition

By definition, an all-optical switch (or all-optical fiber-optic switch if applications in fiber optic links are considered) is a switching device that maintains signal as light from input to

output. In particular, the optical form of signal is maintained regardless of what signal modulation speed or signal transmission protocol.

Traditional switches that connected optical fiber lines were (are) electro-optic. They converted photons from the input side to electrons internally in order to do the switching and then converted back to photons on the output side.

Beside switching optical signals between different outputs (output ports), optical switches may also perform some more elaborate functions like separating signals at different wavelengths (and then directing them to different output ports).

3.14 Evolution, requirements and challenges of optical networks

Below, there are given some general remarks concerning the evolution of current-day optical networks towards an increased utilization of technologies based on all-optical switching.

- o Evolution from point to point WDM links to all-optical networks
- o Requirements for new fiber optic networks

  - o bit rate transparency
  - o protocol transparency

- o Challenge. Optical networking today is hampered by the unavailability of high-performance low-cost optical components. Developing low-cost methods for fabricating large optical switches and tunable lasers is the key to the realization of all-optical networks

3.15 Applications

Optical switches can be employed at different points within optical telecommunication network, i.e. they can perform different functions. Below, there are listed major application areas of optical switches within optical networks.

1. Network protection and reconfiguration (required switching time ~5ms)
2. All-optical networking – circuit switching (WDM networks, OADM's, OXC's)
3. All-optical networking – packet switching (required switching time ~1ns)

Network protection mentioned above includes such functions as passing optical transmission through a different optical link in case one link (optical fiber, optical cable) gets corrupted. Network reconfiguration functionality also changes transmission path but now in response to other reasons (network users' request).

Circuit switching is a general term describing a method of providing transmission channel between two network nodes. In circuit switching, a physical connection is formed between the two nodes. The connection persistence is independent of whether data are exchanged between nodes or not. Moreover, as intermediate network nodes (i.e. nodes along the physical connection that has been formed) do not decode the transmission data as they do not need to e.g. read data destination address from data packets being transmitted. This is why, circuit switching based networks allow the use of any communication protocol between the two communicating nodes without the need of making the intermediate nodes "understand" the given protocol.

Packet switching does not rely on forming a physical connection. Instead, individual packets are routed by the intermediate nodes. Such an approach allows to optimize network resources utilization (no connection is maintained when no data is exchanged by the two communicating nodes). On the other hand, the intermediate nodes need to decode individual data packets in order to forward them to appropriate subsequent nodes. In particular, if transmission channel's bit rate is high, all parameters of intermediate nodes must be good enough to enable data packet decoding. As we know, the higher the network node transmission speed parameters the higher the equipment needed to be installed.

In optical domain, operations needed

3.16 Application example - OADM

Three nodes were interconnected in a unidirectional self-healing two-fiber ring network demonstrator. Nodes are separated by 90 km of standard single mode fiber.
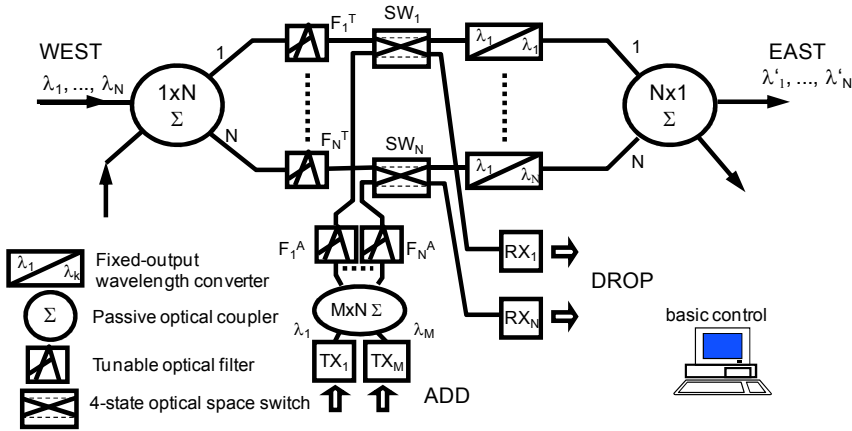
Fig. 3.3 Application example – Optical Add-Drop Multiplexer (OADM).

Example details: 4 wavelength x 2.5 GB/s (STM-16), tunable Fabry–Perot filters, optomechanical switches and 3-R optoelectronic regenerators. All components are commercially available.

3.17 Design requirements for optical switches

Designing an optical switch is not a straightforward task. An optical switch needs to fulfill multiple requirements in order to be practically usable. If such a switch is planned to be employed in fiber optic telecommunication systems, the relevant requirements are:

- o polarization independence,
- o low crosstalk,
- o low insertion-loss or even gain,
- o wavelength independence (in the EDFA wavelength range);
- o multi-wavelength operation,
- o bit-rate transparency – up to at least 10 (40?) Gb/s
- o fast switching,
- o simple implementation,
- o scalability.

Optical switch polarization independence is important due to the fact that standard telecommunication fibers do not maintain light polarization (i.e. light polarization at fiber output differs from that at fiber input). Low crosstalk concerns optical signal leakage (undesired transfer of optical power) from one transmission channel to another. In particular, this can mean a leakage between different wavelengths if WDM channels are considered, or leakage between different output ports of optical switch (such a leakage affects both the WDM and TDM transmission channels). Low insertion-loss is always a desired property of different kinds of optical elements of fiber optic links. The lower the insertion-loss of link's elements, the higher the optical output power which, in turn, allows longer fiber distances to be used (without optical regenerators) and / or enables lower transmission error rates (BER, bit-error rate).

Multi-wavelength operation if the switch is planned for use in WDM telecommunication system carrying simultaneously several wavelength.

Bit-rate transparency is the optical switch ability of transmitting optical signals regardless of their modulation speed. Thus, switch can be applied in different telecommunication systems without a need for adjusting its properties (construction) to modulation speeds (bit rates) present in given system. Fast switching is, in fact, "fast enough", i.e. optical switch need to

complete its switching operation as fast as requirements of any specific application are. Usually, the required switching times vary from several milliseconds to several nanoseconds. By simple implementation we mean a manufacturing process that will be simple enough to result in satisfactory production yield (percentage of functional optical-switch structures out of the entire number of structures produced). If manufacturing process yield is to low, or the process is inherently not suitable for mass production, it cannot be successfully used.

By scalability, we understand possibility to increase the number of users served by a network or the network node. The same requirement applies to active networking devices, in particular to optical switches.

3.18 Classification of optical switches

Designer of optical switches, usually look for physical effects that can significantly change properties of material or structures that can significantly change parameters of the light wave. The list modulators built on of such effects and designs is given below:

1. Thermooptic
2. MEMS
4. Bubble switch (including electrowetting)
3. Integrated optic, electrooptic
4. Acoustooptic
5. Semiconductor switches (with potential for monolithic integration)

3.19 MEMS (MOEMS) Switches

Acronym. MEMS - Micro-electro-mechanical system

The most popular design of optical switch applied in contemporary telecommunications is the MEMS switch. Another popular name is MOEMS, where "O" is for Optical.

Technology. MEMS are miniature devices fabricated with a process called micro machining. The structures range in dimensions from a few hundred microns to millimeters, and are mostly fabricated on silicon substrates, using standard semiconductor processing techniques.

MEMS offer the same potential benefits as large-scale electronic integrated circuits: low-cost and high-volume automated production.

MEMS offer their own challenges:

1. unlike electronic circuits, these are mechanical devices,
2. reliability for telecommunications applications is still to be proved.

3.20 Advantages of using silicon for micro-optical components

In principle different materials can be used to fabricate optical MEMS switch, however currently the material of choice is silicon. The list of reasons is given below:

1. The silicon surface when treated properly can provide an optical surface of extremely high quality (flat and scatter-free).
2. The excellent mechanical properties of single-crystal silicon allow fabrication of fatigue-free devices. Since single-crystal silicon has no dislocations, it has virtually no fatigue and is a perfect elastic material — a property that is extremely desirable for precision mechanics applications.
3. The electrical properties of silicon allow the integration of sensors and detectors with high precision.
4. Silicon is totally transparent at the wavelengths used in optical communications.
5. The lithographic batch-fabrication of these devices, driven and made possible by the existing IC technology, provides a relatively inexpensive fabrication method.

3.21 MEMS Switch architectures

Design of optical MEMS switch can take a form of two-dimensional switch or three-dimensional switch.
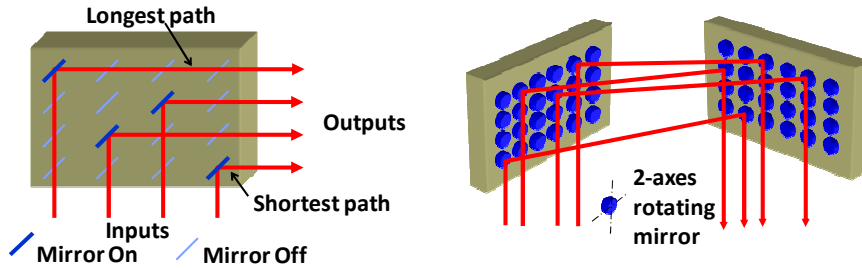
Fig. 3.4 Two dimensional MEMS switch (left) vs. three dimensional MEMS switch (Yeow, Law, & Goldenberg, 2001)**.**

2D MEMS switches

Mirrors are arranged in a crossbar configuration. They can be in either the ON position to reflect light or the OFF position to let light pass uninterrupted. For and NxN-port switch, a total of N2 mirrors is required for strictly nonblocking switching fabric.

3D MEMS switches

The switch has mirrors that can rotate about two axes. Light can be redirected in space to multiple angles. This approach results in N or 2N mirrors (2N mirrors offer lower insertion losses).

3.22 2D MEMS Switch

Example design of 2D MEMS switch is presented in Fig. 3.5.

Mirrors are arranged in a crossbar configuration. Each mirror has only two positions and is placed at the intersections of light paths between the input and output ports. They can be in either the ON position to reflect light or the OFF position to let light pass uninterrupted.
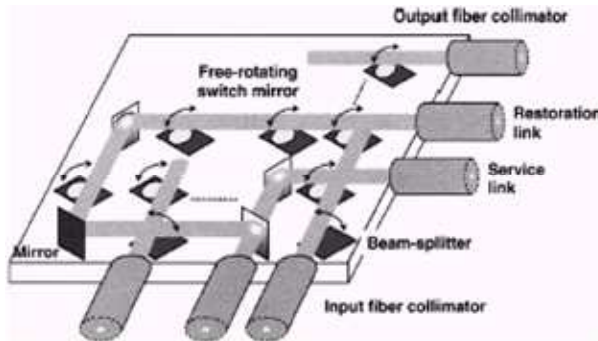
Fig. 3.5 Example design of 2D MEMS switch (Lin, Goldstein, & Tkach, 1999)**.**

Applications: switches with small port counts
Disadvantages:

o   large mirror-count required
o   free space propagation distances are different, which results in different insertion losses for different paths (>5dB).

30

3.23 3D MEMS Switch

Design of 3D MEMS switch is based on mirrors that can direct a light beam in arbitrary direction. 3D MEMS switch illustrated in Fig. 3.6 has mirrors that can rotate about two axes. Light can be redirected precisely in space to multiple angles. This approach results in only N or 2N mirrors.
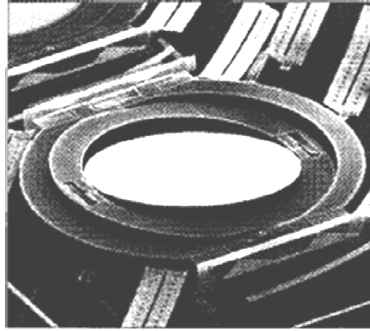
Fig. 3.6 A mirror of 3D optical MEMS switch. The whole structure is based on silicon, and fabricated with silicon processing technologies (Aksyuk et al., 2000)**.**

The 3D MOEMS design is more universal than 2D structure, but technology is significantly more complicated.

3.24 Actuating mechanisms

Every MOEMS switch requires some mechanism to move the mirrors. This mechanisms are called actuating mechanism.

A list of requirements for actuating mechanism for MOEMS:
1. Small
2. Easy to fabricate
3. Accurate
4. Predictable
5. Low power consumption

There are three actuating mechanisms that are currently in use. The list, together with a short description, is given below.

- Electrostatic - attraction forces of two oppositely charged plates.

    - Advantages: well understood, good repeatability.
    - Disadvantages: nonlinearity in force-voltage relationship, high driving voltages

- Electromagnetic - attraction between electromagnets with different polarity.

    - Advantages: large forces with high linearity, low driving voltages.
    - Disadvantages: shielding required to prevent crosstalk, reliability not proved yet

- Scratch drive actuator (SDA): movement controlled by balance of friction and pulsed electrostatic interaction between surfaces.

    - Advantages: no holdup voltage required, movement in small steps (10 nm)

3.25 Scratch-Drive Actuator

The movement principle of SDA is given below, together with a short description
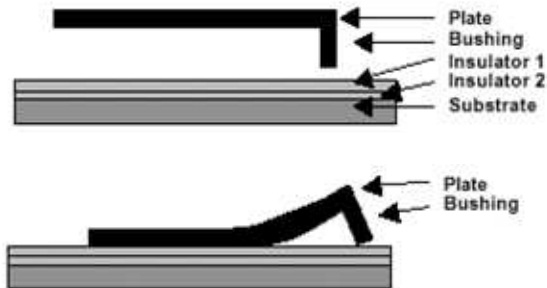
Fig. 3.7 Scratch Drive Actuator – illustration of movement principle (Akiyama & Fujita, 1995)**.**

To drive the SDA:

1. A step voltage load is applied between the substrate and the plate.
2. This results in the unsupported end of the plate snapping to the insulators, pushing the bushing outwards.
3. When the voltage is released, the SDA is moved forward by the bushing.

Example design of SDA-based switch is given in the figure below.
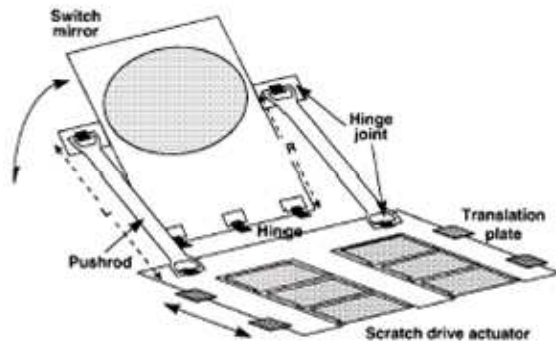
Fig. 3.8 Element of 2D MEMS switch, with SDA engine. Two SDAs are visible to drive the mirror in the opposite directions (Lin, Goldstein, & Lunardi, 2000)**.**

3.26 Active space switches

Active space switches are based on the structure of Semiconductor Optical Amplifier. The unique feature of this class of switches is possibility to compensate for losses.
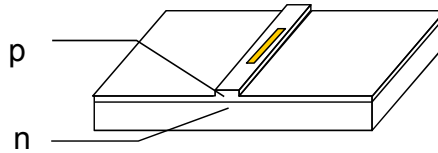
Fig. 3.9 Basic SOA-based switch configuration.

Current injection into semiconductor pn-junctions generates free carriers. This carrier modulation varies the loss and/or gain characteristics. Employing these characteristics, switchable semiconductor optical amplifiers (SOA's) can be realized.
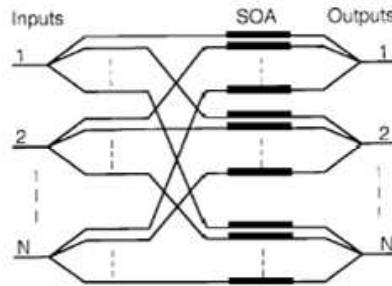
Fig. 3.10 Structure of active optical switch based on SOAs and optical splitters/combiners

4 Fundamentals of nonlinear optoelectronics and optical bistability

4.1 Nonlinear phenomena – definition

Whenever material response (electric polarization, current density, magnetization) is nonlinear function of electrical or magnetic field - nonlinear electromagnetic phenomena appear.

Examples from classical electrodynamics: magnetization curve for ferroelectric materials, Faraday effect (twist of polarization plane in magnetic fields)

Examples of optical nonlinearities: optical harmonic generation, nonlinear refractive index changes.

4.2 Introduction

Usually electrical field strength (E) of optical fields is much lower than internal atomic fields. In such cases, there is a linear relation between electrical field strength (E) and dielectric displacement (D).

$$\vec{D} = \varepsilon \vec{E} \tag{4.1}$$

Nonlinear effects will appear for optical power density of about $1\ kW/cm^2$ $(10^7\ W/m^2)$. Nonlinear optical devices, for their operation, need optical powers one order of magnitude higher. In general, power densities as high are difficult to be attained in a practically usable compact device. However, this problem is alleviated in optical waveguides. Thanks to their small cross-sectional dimensions, high optical power densities are available even for low-power optical beams.

4.3 Power densities in optical waveguides

Below, there are given some general facts concerning optical power and, in particular, concerning optical power in optical waveguides.

Optical power:

- o usually denoted as P
- o usually measured in milliwatts (mW)
- o 1 mW = 10^{-3} W
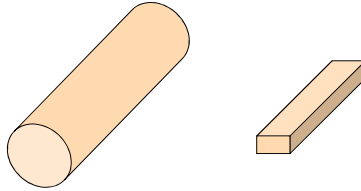
Fig. 4.1 Rough comparison between single-mode fiber (left) and strip waveguide (right) cross-sectional dimensions.

Single-mode optical fibers:

- o mode field diameter (d) 10 µm
- o cross-section area (S) $78.5*10^{-12}$ m^2
- o power density P/S = $1.3*10^7$ W/m^2 – enough power for noticeable nonlinear optical effects to occur

Strip waveguides:

- o width5 µm
- o thickness1 µm
- o cross-section area (S) $5*10^{-12}$ m^2
- o power density P/S = $1.3*10^7$ W/m^2 – enough power for noticeable nonlinear optical effects to occur

4.4 Nonlinear optical effects

The field of nonlinear optics has been under strong development since the 1960s. Research areas include:

- o   harmonic frequency generation
- o   nonlinear spectroscopy (e.g. Raman)
- o optical phase conjugation
- o optical bistability
- o optical switching

4.5 From the history of nonlinear optics ...

A pioneering work of P. A. Franken (P.A. Franken, A.E. Hill, C.W. Peters, G. Weinreich, Phys. Rev. Lett., vol. 7 (1961), no. 4, pp. 118-119) – a proof which is not there.

FIG. 1. A direct reproduction of the first plate in which there was an indication of second harmonic.

Fig. 4.2 „Fig. 1. A direct reproduction of the first plate in which there was an indication of second harmonic. The wavelength scale is in units 100 A. The arrow at 3472 A indicates the small but dense image produced by the second harmonic. The image of the primary beam at 6943 A is very large due to halation." (Franken, Hill, Peters, & Weinreich, 1961)**.**

4.6 Constitutive equation (nonlinear optics)

Nonlinear optical effects and devices are analyzed with Maxwell's equations – just as linear optical systems. However, this time one has to take into account dependence of material properties on electrical field strength. This is done with constitutive equations of Maxwell's equations set. In classical optics, permittivity does not depend on power, so the equations are written in the following form:

$$\vec{D} = \varepsilon \vec{E} = \varepsilon_0 \vec{E} + \vec{P} \tag{4.2}$$

$$\vec{B} = \mu \vec{H} = \mu_0 \vec{H} + \vec{M} \tag{4.3}$$

$$\vec{B} = \mu \vec{H} = \mu_0 \vec{H} + \vec{M} \tag{4.4}$$

In more general case, to describe nonlinear optical response of the material, one has to include a nonlinear term into equations. In the equation (4.5) nonlinear polarization is   to describe nonlinear response of the material (Liu, 2005).

$$\vec{D} = \varepsilon \vec{E} = \varepsilon_0 \vec{E} + \vec{P}_L + \vec{P}_{NL} \tag{4.5}$$

$$\vec{P}_L = \varepsilon_0 \chi_L \vec{E} \tag{4.6}$$

$$\vec{P} = \varepsilon_0 \chi_L \vec{E} + \vec{P}_{NL} \tag{4.7}$$

4.7 Nonlinear refractive index

Material response for optical beam propagation is characterized by polarization vector **P** and dielectric susceptibility tensor χ.

$$\mathbf{P} = \varepsilon_0 \chi(\mathbf{E}) \mathbf{E} \tag{4.8}$$

If the atomic vibration amplitude is high enough, response is becoming nonlinear. Nonlinear response is described by higher order terms in the power series (Liu, 2005)

$$P = \varepsilon_0 \left(\chi^{(1)} E + \chi^{(2)} EE + \chi^{(3)} EEE + \cdots + \chi^{(n)} E^n + \cdots \right) \tag{4.9}$$

Consecutive components of the sum in (4.9) are responsible for: linear optical effects, 2-nd order nonlinear optical effects, 3-rd order nonlinear optical effects, and so on. In most cases, only the three first components are of interest in practical applications. The second order and third order effects are commonly referred to as Pockels and Kerr effects, respectively.

Some more details will be given in paragraph 4.8. Let us only mention here, that in second order effects, material refractive index depends on the electric field value. In third order effects,

material refractive index depends on optical power, which is proportional to the square of the electric field.

4.8 Classification of optical nonlinear effects

Refractive index n of material showing third-order nonlinearity is given by

$$n = n_0 + n_2 \langle E^2 \rangle = n_0 + \frac{1}{2} n_2 E^2 \qquad (4.10)$$

where: n_0 is a linear refractive index, n_2 is a third order refractive index, and E denotes strength of the electric field. Angled brackets mean the time averaging of electric field values (harmonic oscillations of the electric field are assumed).

In cases when light power is given in terms in optical power density I ([W/m^2]) instead of electric field value E ([V/m]), the formula (4.10) takes the following form

$$n = n_0 + n_2' E^2, \ n = n_0 + n_2'' I \qquad (4.11)$$

Both types of the third-order nonlinear refractive index present in (4.11), i.e. n_2' and n_2'', can easily be converted to each other by means of the following formula

$$n_2 = 2n_2' = \left(\frac{cn_0}{4\pi} \right) n_2'' \qquad (4.12)$$

For completeness, let us also write a relation between n_2 (see (4.10)) and the third order dielectric susceptibility $\chi^{(3)}$

$$n_2 = \frac{3}{4\varepsilon_0 cn^2} \chi^{(3)}(-\omega; \omega, -\omega, \omega) \qquad (4.13)$$

4.9 Nonlinear optical materials – selecting criteria and figures of merit

Nonlinear materials can be characterized by their respective nonlinear parameters, e.g. Nonlinear susceptibility or nonlinear refractive index. However, for the purpose of comparing different materials for different applications, additional parameter is introduced. This parameter is called "figure of merit" (Stegeman, 1993). Figures of merit are defined in different ways for second order and third order nonlinear effects.

Nonlinear second order figure of merit:

$$M_{ij} = d_{ij}^2 / \left(n_\omega^2 \ n_{2\omega} \right) \qquad (4.14)$$

where d_{ij} is nonlinear optical coefficient of the second order, and n_ω and $n_{2\omega}$ are refractive indices for first and second order beams, respectively.

Nonlinear third order figure of merit:

$$M_1^{\chi^{(3)}} = \frac{n_2}{\lambda \alpha} \qquad (4.15)$$

Often, above certain field strain, nonlinear effect is saturated.
Saturated figure of merit is defined as:

$$M_{sat} = \frac{n_2^{sat}}{\lambda \ \alpha} \qquad (4.16)$$

where n_2^{sat} is saturated third order refraction index

In the tables below nonlinear parameters and figures of merit for second and third order nonlinearities are given.

Table 4.1 Parameters and figures of merit of selected materials for 3rd order nonlinearities

Material	λ	Nonlinear refractive index n_2	Response time τ	α	$n_2/\lambda\alpha$	Δn_{sat}	$\Delta n_{sat}/\lambda\alpha$
	μm	m^2/W	s	1/cm	x10^{-8}		
GaAlAs [r]	1	10^{-8}	10^{-8}	10^4	1	0,1	0,1
GaAlAs [nr]	1	10^{-12}	10^{-8}	30	0,033	2×10^{-3}	0,9
Sd CdS$_x$Se$_{1-x}$	1	10^{-14}	10^{-11}	3	0,003	5×10^{-5}	0,3
PTS [nr]	1	$>10^{-16}$	$<10^{-12}$	<2	5×10^{-5}	$>10^{-3}$	>10
SiO$_2$	1	10^{-20}	10^{-14}	10^{-5}	10^{-3}	$>10^{-6}$	>1000

Table 4.2 Parameters and figures of merit of selected materials for 2nd order nonlinearities.

Material	λ [nm]	n_ω	$n_{2\omega}$	nfm (*) [x10^{-24} m^2/V^2]	Damage threshold [GW/cm^2]	Bandwidth [nm]
Kwarc	1064	1,5341	1,547	0,028	1,2	
KDP	1058	1,4938	1,4705	0,029	1,0	200-1500
KD*P	1058	1,4978	1,4689	0,034	0,7	200-1500
ADP	1058	1,5066	1,4815	0,041	0,4	200-1200
LiNbO$_3$ d$_{31}$	1058	2,2322	2,2325	1,84	0,1	350-4500
LiNbO$_3$ d$_{33}$	1152	2,1506	2,2153	89,69		
LiTaO$_3$	1058	2,1366	2,2089	0,11		
BBO	1064	1,657	1,5541	0,29	13	190-3500
KTP	1064	1,74-1,83	1,79-189	9,35	0,65	350-4500
LBO	1064	1,566-1,606	1,579-1,621	0,45	25	160-2600
KNbO$_3$	1064	2,21-225	2,20-2,32	10,24		310-5500
LiJO$_3$	1064	1,86	1,75	2,09		310-5500
ZnO	1058	1,95	2,048	0,4		

* Nonlinear figure of merit $d_{eff}^2 / n_\omega^2 n_{2\omega}$

Material Names and abbreviations used in the tables

- o KDP - potassium dihydrogen phosphate, KH2PO4
- o KTP - Potassium Titanyl Phosphate KTiOPO4
- o ADP - Ammonium phosphate NH4H2PO4
- o BBO - beta-Barium Borate BaB2O4

4.10 Organic materials

There are a number of organic materials, with nonlinearities significantly higher than their inorganic counterparts. This materials and their nonlinearities are compared in the figure below. However, it must be noted, that these materials are not in common use because of their low optical damage threshold.

Fig. 4.3 Organic materials and their 2nd order nonlinearities.
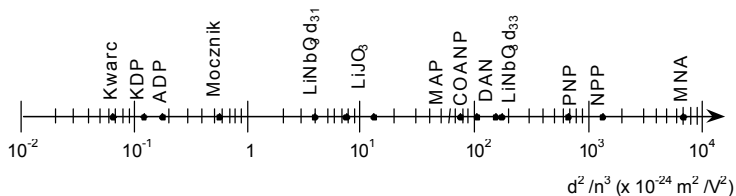
ADP = NH$_4$H$_2$PO$_4$

KDP = KH$_2$PO$_4$

MNA = 2-metylo-4-nitroanilina

NPP = N-(4-nitrofenyl)-(L)- prolinol

PNP = 2-(N-prolinol)- 5-nitropyrydyna

MBANP = 2-(? - metylo- benzyloamino)-5-nitropyrydyna

DAN = 4-(N, N-dimetylo- amino)-3- acetamido-nitrobenzen

COANP = 2-cyclooctyl- amino-5- nitropyrydyna

MAP = 3-methyl-(2,4- dinitrofenylo)- amino-propanol

POM = 1-tlenek 3-metylo-4-nitro-pyrydyny

4.11 Simple all optical M-Z interferometer

Probably the simplest way to build nonlinear optical device, is by adaptation of classical electrooptic modulator. The difference consists in replacement of electrical-field stimuli with optical light beam. Example of such optical modulator is shown in Fig. 4.5
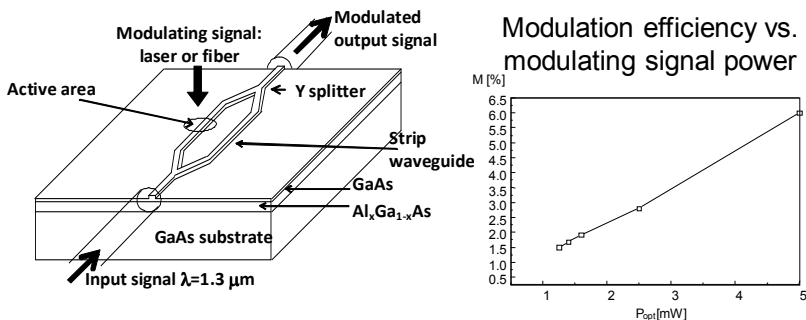
Fig. 4.5 Optical modulator based on Mach-Zehnder interferometer (Łowkis, 1997).

4.12 Phase adjustment condition for nonlinear optical phenomena

Efficient nonlinear interactions often require phase adjustment between interacting beams. In classical optics adjustment is obtained by control of refractive index (e.g. with temperature) of the guiding structures. In integrated optical structures, phase adjustment can be performed through manipulation and adjustment of propagation constants of different modes. E.g. first harmonics and second harmonics beams can be propagated as different modes of a strip waveguide. The effect of phase adjustment through utilization of different modes is illustrated in the following figure. An efficient waveguide device for second harmonic generation is presented in Fig. 4.10.

38
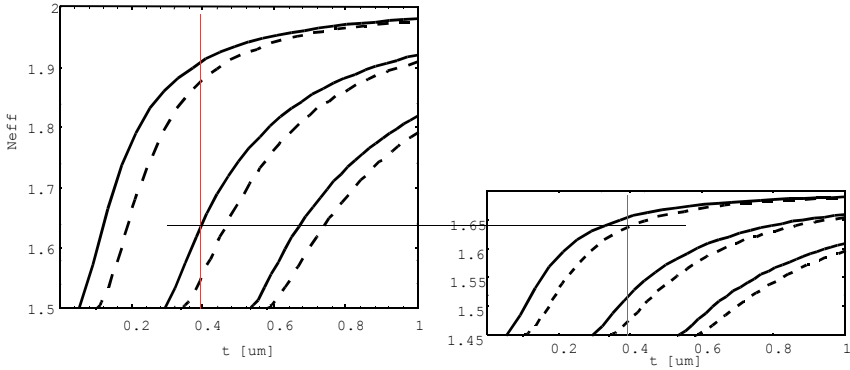
Fig. 4.9 Illustration of phase adjustment of two beams in nonlinear second harmonic generation effect.
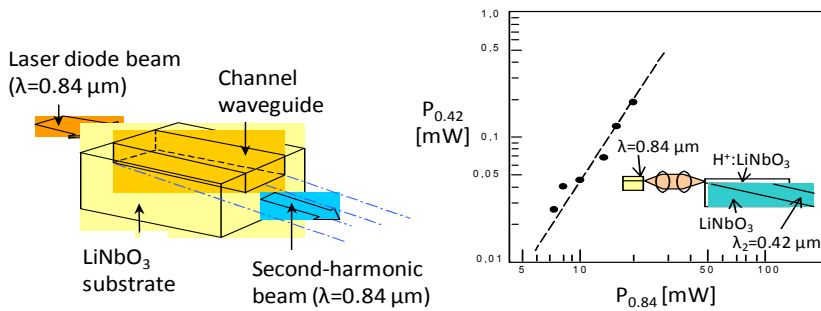
Fig. 4.10 Phase adjustment for efficient second harmonic generation obtained through adjustment of propagation constant of different modes.

4.13 Examples of 3rd order nonlinear integrated optical devices

Several nonlinear integrated optical devices have been build, the list includes:

- o Nonlinear optical logical devices (optical gates)
- o Nonlinear beam deflectors
- o Nonlinear Bragg gratings
- o Nonlinear directional couplers

It is also possible to build nonlinear optical devices with optical fibers, the most notable device here is nonlinear optical loop mirror (NOLM)

Function XOR		
A	B	Q
0	0	0
1	0	1
0	1	1
1	1	0
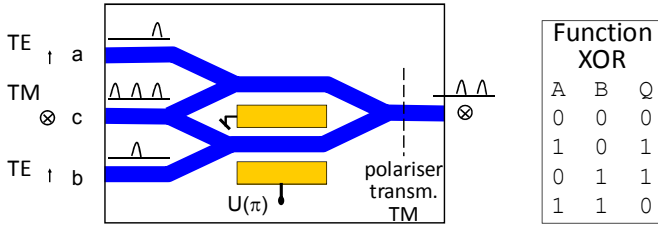
Fig. 4.11 Integrated optical XOR gate. Optical power guided in a and b branches, controls transmission of pulses from the branch c. Electrodes adjust working point of the device (initial phase shift between the branches = π).

Optical power guided in a and b branches, controls transmission of pulses from the branch c. Electrodes adjust working point of the device (initial phase shift between the branches = π).
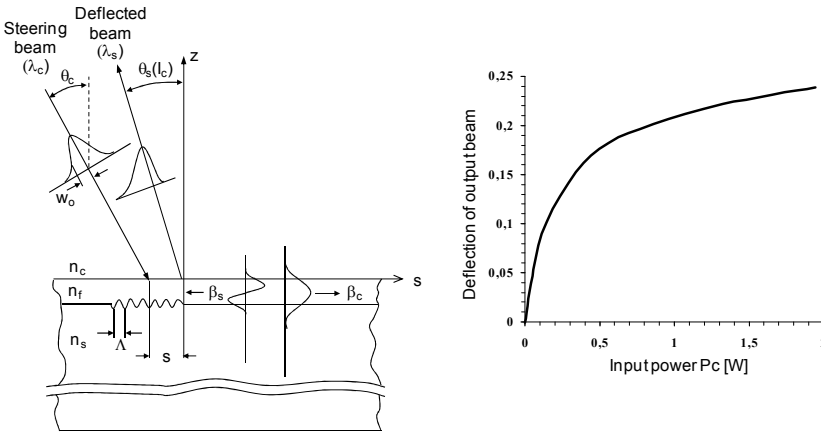
Fig. 4.12 Nonlinear beam deflector.
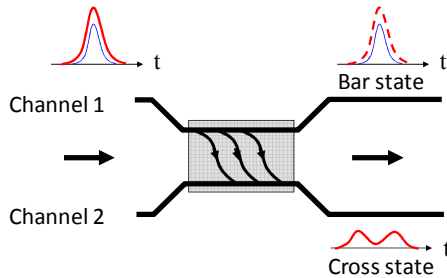
Fig. 4.13 Nonlinear directional coupler. A dashed line depicts operation of a linear device.

40
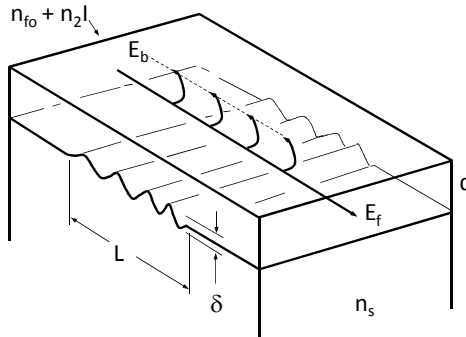
Fig. 4.14 Nonlinear Bragg grating. Bragg condition: 2Λ = νλ, ν = 1,2,3,..., light wavelength λ = λ$_0$ / $n_{waveguide}$, efficient reflection only for λ$_0$ = 2 Λ n$_{waveguide}$ / ν.

5 Optical Measurement Methods

5.1 Semiconductor optical measurement methods

Among the most popular semiconductor-characterization methods are the following:

- o Profilometry
- o Ellipsometry
- o Microscopy
- o Spectroscopy UV, VIS, IR and FIR
- o Photoluminescency
- o Absorption, reflection measurements
- o LBIC

5.2 Optical Profilometry

The visible-light interferometry, also known as the optical profilometry, is one of the contactless measurement methods utilized in metrology for surface roughness measurements and for surface topography investigation. There are multiple scientific as well as industrial applications possible of optical profilometry. It is due to the following features of the method: accuracy, speed, and repeatability.

Profilometer a device for measuring the surface profile.

Optical profilometry is a notably versatile method capable of measuring such geometrical and surface parameters like:

- o waviness
- o roughness
- o roundness
- o form deviation
- o dimensions

There exist a number of profile detection optical methods that are employed in optical profilometry:

- o oscillating lens
- o laser triangulation
- o light section method
- o interference
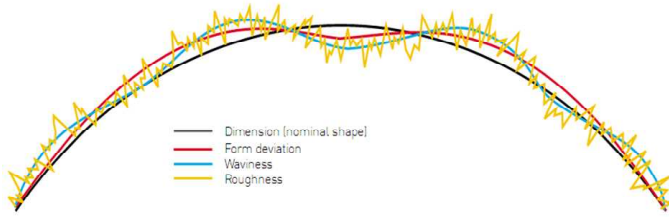
Fig. 5.1 Definitions of some of the surface parameters ("Form Talysurf Brochure," 2010)**.**

5.3 Interference optical profiler

Figure Fig. 5.2 presents a working principle of the interference optical profiler, i.e. the one in which the interference-based profile detection method is employed. Light beam from a light source is split by a semi-transparent plate. One part of the beam, after passing an objective lens, is reflected off the sample surface and returns along the same path. The second part of the beam passes a plate that compensates optical path differences and then, after being reflected off a mirror, it returns along the same path. Once the two beams (i.e. the two parts of the input beam) meet at the semi-transparent plate again, optical interference occurs. Interference fringes can then be observed through an eyepiece furnished by the device.

Height of a surface vertical feature under measurement is calculated according to the formula

$$R = \frac{\lambda}{2} \frac{\Delta L}{L} \qquad (5.1)$$

where: λ — light wavelength, ΔL — fringe lateral shift, L — distance between neighboring fringes. Depending on the construction type, the ΔL and L parameters are measured either with micrometer barrel or by visual inspection. Also taking a photograph is often an option. By using microinterferometers, surface vertical features of the height of $0.03 - 1$ μm can be measured.
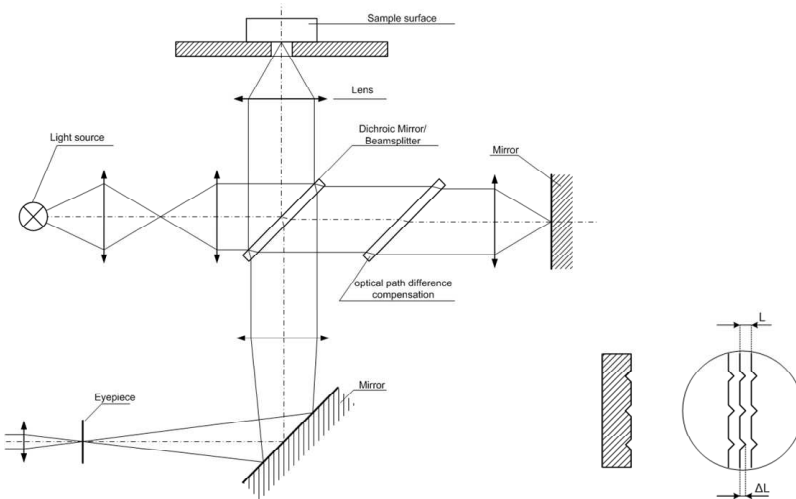
Fig. 5.2 Working principle of the interference optical profiler.

The most significant advantages offered by optical profilometers are:

o Measurement of three-dimensional geometric parameters.
o Precise measurements of small surfaces.

42

o Mapping complex structures.
o Measurements of the surface of susceptible to mechanical damage.
o Thickness measurements of optical thin films.

There are, however, also several limitations characteristic of the optical profilometry. The basic difficulties one should take into consideration when planning to work with an optical profilometer, are:

o Relatively long measurement time.
o Difficulty in measuring strongly light absorbing surfaces (ceramic, photovoltaic modules).
o Problems with the measurement extremely different refractive index (silver on ceramic).
o Measurement of steep slopes limited by the aperture of used lens.

5.4 Ellipsometry

Before we get into a more detailed discussion of ellipsometry, we first need to remind ourselves about some basic ideas concerning the light propagation and the light-matter interaction.

5.4.1 Light polarization

Light is an electromagnetic wave, i.e. an oscillation variation of both the electric (E) and the magnetic (H) field vector values that travels (propagates) across space. Directions of both the field vectors are orthogonal to each other and to the direction of propagation (when propagation is in free space). Thus, the electromagnetic wave of light is a transverse wave. In expressing the electromagnetic wave orientation, direction of the electric field vector is used and it is called the polarization direction.

When distribution of the E and H oscillation directions is not well defined, we have the unpolarized light (unpolarized electromagnetic wave). Once oscillation directions are completely or partially ordered, then the wave becomes polarized.
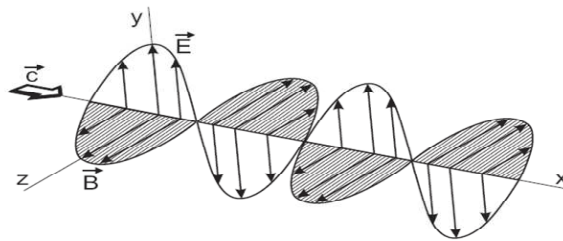
Fig. 5.3 Electromagnetic wave propagation.

A polarized electromagnetic wave can be produced in the following ways (Hecht & Zajac, 1997):

o selective emission – wave source oscillates in one direction only,
o selective absorption – a medium that the wave goes through, absorbs waves of one polarization, but waves of orthogonal polarization are passed through,
o single scattering – an orthogonal-direction scattering generates a polarized wave,
o reflection off a transparent medium – once light hits a boundary between two different transparent media at an appropriate angle (the Brewster's angle), the reflected portion of the original light beam becomes completely polarized. At angles different from the Brewster's angle, the reflected light is partially polarized. The bigger the deviation form the Brewster's angle, the lower the polarization

degree. (As a reminder, in the Brewster's angle reflection, there is an angle of 90° between the reflected and the transmitted beams).
  o birefringence (also called the double refraction).

Three fundamental states of polarization of light are considered (also see figure Fig. 5.4) (Hecht & Zajac, 1997):

  o linear polarization – oscillations take place along a straight line. All kinds of oscillations can be expressed as a sum (superposition) of oscillations along the X- and the Y-axis. In the case of linear polarization, the two oscillation components are either in phase or are 180° out of phase. The ratio of the component oscillation amplitudes determines the direction of the resultant oscillation, thus the polarization.

  o circular polarization – this kind of oscillation corresponds to a circular movement. It can be decomposed into two oscillation components that have identical amplitudes but their oscillations are out of phase by exactly 90° or 270° (-90°). Depending on the case being realized, i.e. 90° or 270°, one talks about the right-hand circular polarization or the left-hand circular polarization, respectively. In the circular polarization, the value of the electric displacement vector (electric flux density vector) remains constant, only its direction varies.

  o elliptical polarization – it is a generalization of the circular polarization. An oscillation-generating body moves along an elliptical path. Similarly to the circular polarization case, the elliptically polarized oscillation can be decomposed into two component oscillations being 90° or 270° out of phase, but having different amplitudes. The elliptical polarization can be expressed as a sum (superposition) of the linear and the circular polarization.
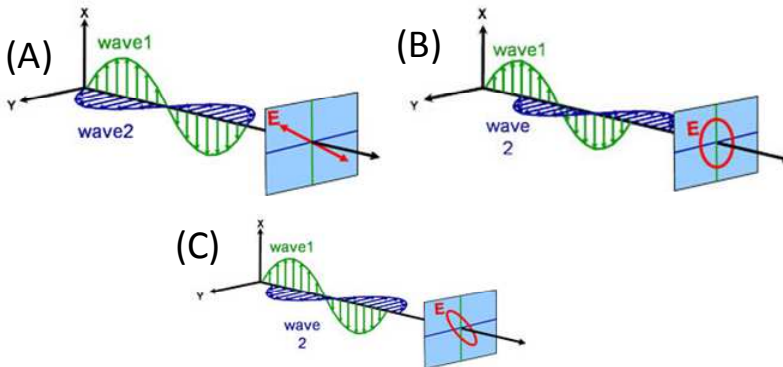
Fig. 5.4 Fundamental states of polarization of light, A – the linear polarization, B – the circular polarization, C – the elliptical polarization ("Ellipsometry Tutorial," 2010)**.**

5.4.2 Ellipsometry – operating principle

Ellipsometry is an analytical technique used for the determination of the optical properties of the surface and of surface morphology. In ellipsometry, changes in polarization of light that has been reflected off the sample surface, are measured. The method relies on correlating the physicochemical properties of the material under investigation with the two parameters, delta and psi, that describe the so called polarization ellipse (Tompkins & Irene, 2005).
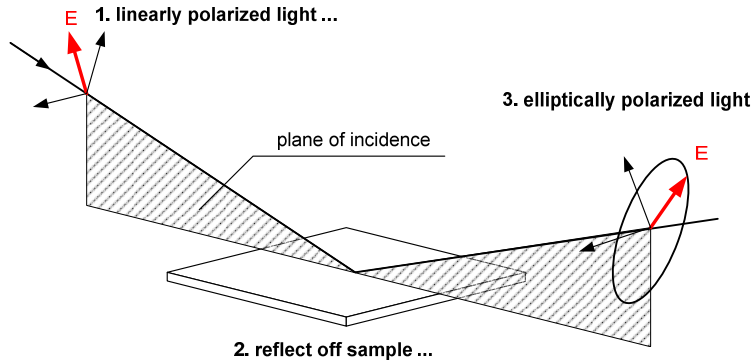
Fig. 5.5 Illustration of the polarization change of light reflected off sample surface – the working principle of an ellipsometer (based on ("Ellipsometry Tutorial," 2010)**).**

By means of measuring the polarization change of light reflected off sample surface, the determination of a thin film thickness (*t*) and optical constants (*n* and *k*). For a given configuration (pair of values) of light wavelength and the angle of incidence, the change in the polarization state of light is described by the following parameters (Tompkins & Irene, 2005):

     o   Delta (Δ)

$$\Delta = \delta_1 - \delta_2 \tag{5.2}$$

     o   Psi (Ψ)

$$\tan(\Psi)\cdot e^{i\Delta} = \frac{R_p}{R_s} = \rho \tag{5.3}$$

The equation (5.3) is known as the fundamental equation of ellipsometry.

Ellipsometry is a noninvasive technique of thin film investigation. Data extracted directly form this method usually require some further analysis steps. Numerical values of parameters like film thickness or film refractive index, need to be computed. The measurement data interpretation requires the assumption of some optical model. Parameter values computed using the model are then fitted to the parameter values extracted directly from measurements. More precisely, in an optimization routine (parameter fitting routine), the difference between both the parameters sets is attempted to be made as low as possible. Such a model fitting is based on software-implemented fitting algorithms. The process of fitting the modeled characteristics to the measured ones is depicted in figure Fig. 5.6. In the process presented, thin film thickness and refractive index are being determined.
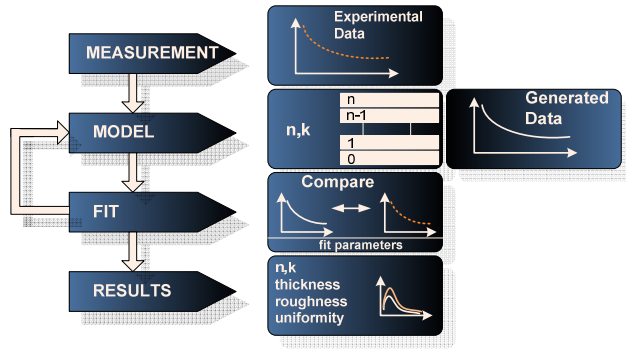
Fig. 5.6 Block diagram of a parameter fitting routine leading to the determination of sample properties (parameter values) based on the ellipsometric data (based on ("Ellipsometry Tutorial," 2010)**).**

Between the ellipsometric measurements and the simple transmission or reflection measurements, there exist some significant differences that make ellipsometry more advantageous in many applications. The differences are listed below.

- o The ellipsometric measurement outcome is always defined in terms of dividing one quantity by some other quantity, i.e. as a ratio – thus sensitivity to light source power fluctuations (instabilities) is eliminated.
- o By considering also the phase information (instead of only the amplitude information), sensitivity of ellipsometric measurement can be pushed down to ultra-thin films (sub-nanometer thickness).
- o An ellipsometer measures two quantities (parameters), Δ and Ψ, for every value of light wavelength – this means the amount of information being extracted from measurements is doubled compared to the simple transmission or reflection measurements.

Ellipsometric measurements are capable of the determination of the following parameters of sample layers being investigated:

- o refractive index
- o thickness of layers (including thin films)
- o roughness
- o homogeneity
- o composition

46

5.5 Optical Microscopy
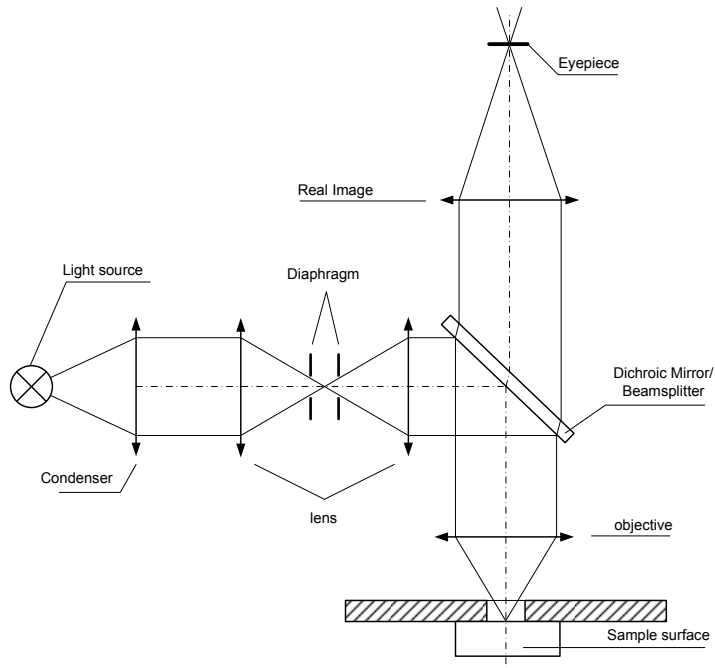
Fig. 5.7 Schematic of the optical light microscope.

The optical microscope working principle is explained in figure Fig. 5.7. Light beam from a light source enters a condenser and leaves it as leaves it as a collimated beam of high intensity. Then the beam passes an aperture diaphragm that reduces the overall optical power level, but increases the optical field depth. The so prepared light beam reaches a semi-transparent mirror and then, by means of an optical objective, it is focused on sample surface. After being reflected off the surface, the light beam returns along the same path, i.e. it passes the semi-transparent mirror again. Then, the image is cast into the eyepiece.

Microscope image spatial resolution is inherently limited. To precisely express (quantify) this limitation, the Rayleigh criterion is used. As illustrated in figure Fig. 5.8, the criterion states that images of two different points can be regarded as separate (resolvable) when the principal diffraction maximum of one image coincides with the first diffraction minimum of the other image.
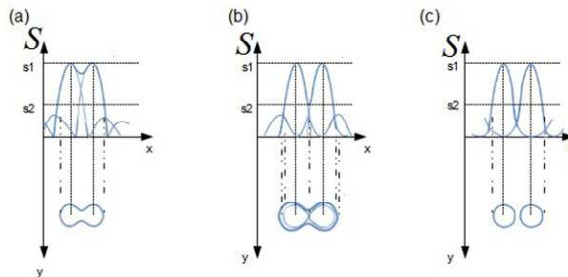
Fig. 5.8 Diffraction characteristics of test images: (a) below spatial resolution, (b) equal to spatial resolution, and (c) above spatial resolution of optical setup.

The spatial resolution of a microscope – the shortest distance *l* between two black lines that can still be resolved, in Rayleigh's sense, by the eye. For a given optical objective, with the assumption that monochromatic light is used, the shortest distance is expressed with the formula

$$l = \frac{0{,}61 \cdot \lambda}{NA} \tag{5.4}$$

where

$$NA = n \cdot \sin \alpha \tag{5.5}$$

n – refraction index of the object space, α – object aperture angle, λ – light wavelength.

The formula (5.4) is correct provided that the objective and the condenser numerical aperture values are equal. Otherwise, a different formula needs to be applied

$$l = \frac{1{,}22 \cdot \lambda}{NA_{Ob} + NA_{Kon}} \tag{5.6}$$

where NA_{Ob} – objective numerical aperture, NA_{Kon} – condenser numerical aperture.

The objective resolution can be increased by means of illuminating the sample (object) with light of a wavelength shorter than that of the visible light. Alternatively, increasing the numerical aperture can be utilized.

The microscopic investigation methods are listed below.

- o Bright field illumination – the most frequently used illumination method. The resulting image has dark, thin contours visible on bright background. This method gives maximal resolution due to taking full advantage of microscope numerical aperture. However, the semitransparent plate introduces optical loss.
- o Dark field illumination – a method giving, in a certain sense, opposite results as compared to the bright field illumination. The resulting image has bright details on dark background. In this method, microscope numerical aperture is fully utilized as well.
- o Cross-polarized light.
- o The phase contrast and interference – used when specimens under observation give no changes in the reflected light amplitude but only introduce the reflected light phase variations.
- o At raised and reduced temperatures – measurements of melting and freezing temperatures (possible thanks to high surface tension).
- o Fluorescent.
- o The IR radiation.

Optical microscopy is also commonly utilized in determining the following parameters of specimens under investigation:

- o surface topology
- o geometrical dimensions
- o surface condition

5.6 Spectroscopy

Spectroscopy is a field of science, which includes research matter methods using electromagnetic radiation, which can be produced in a given system (emission), or may interact with this system (absorption).

Spectroscopy classifications are usually done according to the following criteria (Kurzak, 2010):

- o electromagnetic radiation range (i.e. range of supported radiation wavelengths)
- o properties of physical systems being investigated

o radiation source type

Classification of spectroscopy according to the range of radiation (Kurzak, 2010):

o	Space Spectroscopy	10^{-5} - 10^{-3} Å
o	Gamma spectroscopy	10^{-3} - 1 Å
o	X-ray spectroscopy	1 - 10^2 Å
o	Optical spectroscopy	

o	in the near and vacuum ultraviolet range	100 - 300 nm
o	in the visible range	360 - 800 nm
o	in the near, medium, far-infrared	0.8 - 15 μm

o Radio spectroscopy

o	in the microwave range	0.03 - 100 cm
o	short-range	10 - 100 m
o	long-range	100 - 4000 m

Classification of spectroscopy according to the physical system properties:

o Nuclear Spectroscopy
o Atomic Spectroscopy
o Molecular Spectroscopy

Classification of spectroscopy according to the radiation source type:

o Absorption spectroscopy
o Reflectance spectroscopy (including modulating spectroscopy)
o Emission spectroscopy
o Raman spectroscopy

5.6.1   Beer-Lambert law
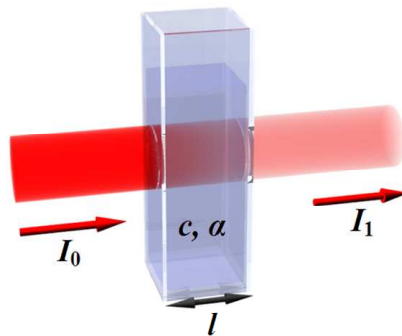
Fig. 5.9 Illustration of Beer-Lambert law description of optical absorption ("Beer-Lambert Law," 2010)**.**

Beer-Lambert states that for a plane, strictly monochromatic beam of electromagnetic radiation, in the case of a non-absorbing solvent, when there are no interactions between absorber particles or between absorber and solvent particles, absorbance A is proportional to the solution concentration c and the thickness of the absorbing layer l

$$A = \log \frac{I_0}{I_1} = \varepsilon l c \tag{5.7}$$

49

$$\varepsilon = \alpha \cdot \log e \qquad (5.8)$$

where: ε – molar absorptivity of the absorber, and α – absorption coefficient of the substance.

5.6.2   Absorbance additivity law

Absorbance additivity law concerns multi-component solutions and mixtures. It states that the total absorbance is the sum of absorbances of individual components (substances) (A_1, A_2, ..., A_n) (Kurzak, 2010)

$$A = A_1 + A_2 + ... + A_n = \sum_{i=1}^{n} A_i \qquad (5.9)$$

Formula (5.9) can only be applied in situations when individual components do not interact (no chemical interactions) thus each of the components absorbs light individually.

One of absorbance additivity law applications is to subtract spectra of individual solution / mixture components from a total spectrum measured for the solution / mixture as a whole. An example of such a subtraction is given in figure Fig. 5.10.
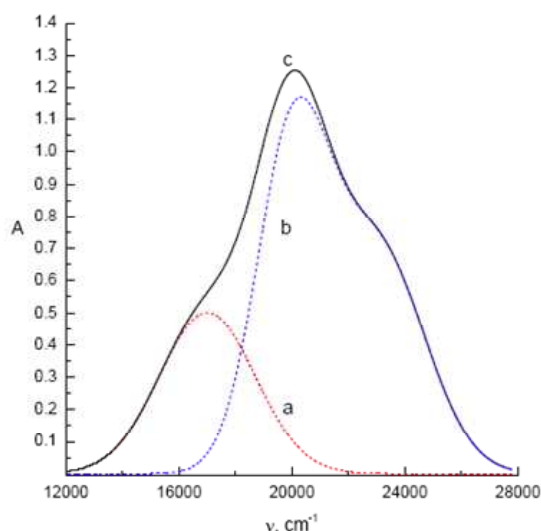
Fig. 5.10 Illustration of absorbance additivity law: *a* + *b* = *c*, where a and *b* are spectra of individual solution / mixture components (substances) and *c* is the total absorbance spectrum, i.e. the one measured for the solution / mixture as a whole (Kurzak, 2010)

5.6.3   FTIR spectroscopy – Michelson interferometer

A key element of Fourier-transform infrared spectroscopy (FTIR) measurements is Michelson interferometer (also see paragraph 5.6.4). Principle of operation of the interferometer is displayed in figure Fig. 5.11. Michelson interferometer contains two mirrors positioned at an angle of 90° to each other. Whereas one of the mirrors is fixed in its position, the second mirror is mounted so that its position can be shifted. Light generated by a light source reaches a semitransparent mirror and it is split into two separate beams. The beams, after being reflected off the movable and the immovable mirror surfaces, reach a photodetector. Now, in case the movable mirror is shifted by a distance *x* then optical path difference (between both the beams) at the detector will change by 2*x*.
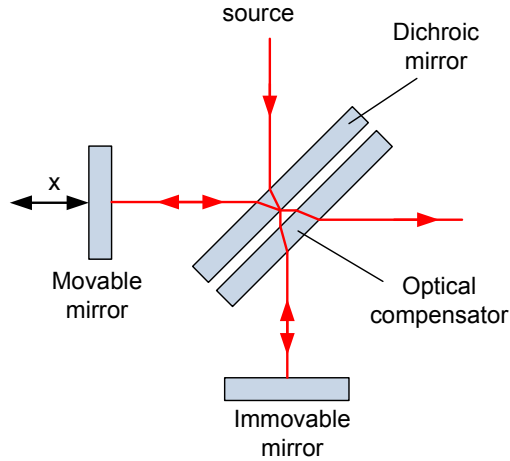
Fig. 5.11 Michelson interferometer – principle of operation.

5.6.4 FTIR spectroscopy

A schematic view of a FTIR spectroscopy measurement setup, a FTIR spectrometer, is shown in figure Fig. 5.12. Michelson interferometer, discussed in 5.6.3, is one of setup's elements. Among other elements there is a He-Ne laser employed as a reference light-beam source. Two mirrors visible in the picture feature holes purposely drilled at their centers to allow passing the reference light-beam. At certain parts of the FTIR setup, both the reference and the IR beams run parallel to each other.
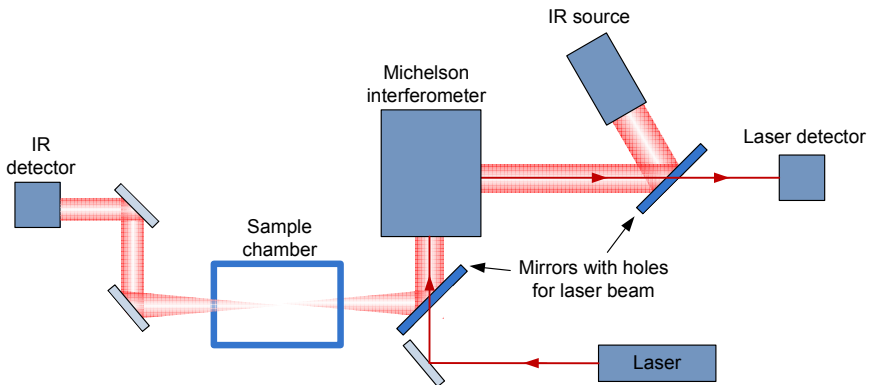
Fig. 5.12 Fourier-transform infrared spectroscopy (FTIR) measurement setup – construction details (based on (Szroeder, 2010)**).**

In the semiconductor-related research area, by means of FTIR spectroscopy, absorption spectral characteristics of semiconductor materials can be determined. Moreover, measurements of the following parameters commonly used in semiconductor characterization are feasible with FTIR:

- o shallow donor energy levels
- o dopant concentration
- o carrier effective masses
- o carrier mobilities

o   thickness of multilayer structures

Also detailed investigation of crystal lattice vibrations are possible.

5.7 Refractometry

5.7.1 Snell's Law

On passing a boundary between two different dielectric media, light beam is refracted. The reason of refraction is a difference between light propagation speeds (group velocities) in both the media as it is schematically shown in figure Fig. 5.13. Such a behavior of the electromagnetic wave is mathematically expressed with Snell's law. Snell's law states that the incident beam and the surface normal (i.e. direction perpendicular to the surface) lie in the same plane. Ratio of the values of the sine function calculated for the incidence angle α and for the refraction angle β, equals the ratio of light speeds in both the media, i.e. v_1 and v_2

$$\frac{\sin \alpha}{\sin \beta} = \frac{v_1}{v_2} \tag{5.10}$$

$$\frac{\sin \alpha}{\sin \beta} = \frac{n_2}{n_1} \tag{5.11}$$
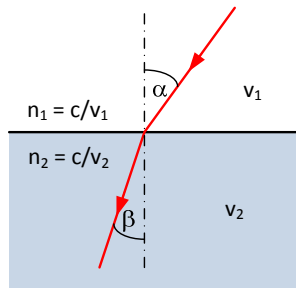
Fig. 5.13 Light refraction at dielectric boundary.

5.7.2 Abbe refractometer

Principle of operation of Abbe refractometer is shown in figure Fig. 5.14. Key elements of the refractometer are two rectangular prisms positioned so that their sides (hypotenuses) are parallel to each other and a gap is created between them. The gap is then filled with investigated substances during measurements. Light from a light source hits a matte surface (prism hypotenuse) of the first prism and it is diffused. After reaching a boundary between the substance and the second prism, light undergoes refraction and only a beam limited by the critical angle enters the second prism. After emerging from the second prism, light beam is directed by a mirror onto a special linear scale. The critical beam is reflected off the mirror surface at a maximum angle and a bright area and a dark area appear on the scale. Position of the bright-dark field boundary depends on the critical angle. The critical angle, in turn, depends on the investigated substance's refractive index.
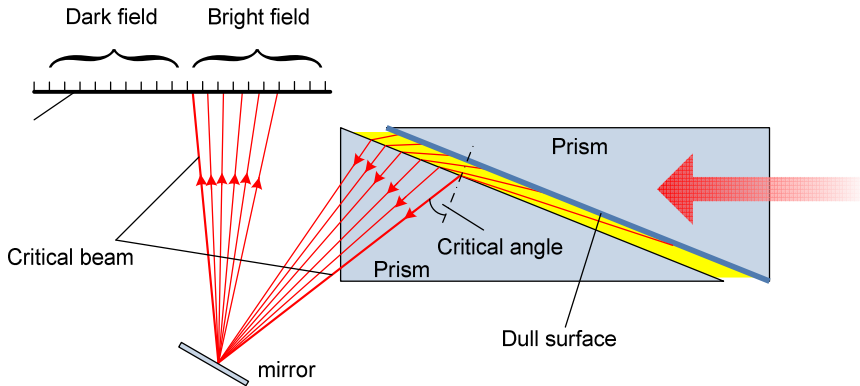
Fig. 5.14 Abbe refractometer principle of operation (based on (Rebilas, 2010)**).**

Refractometry allows determination of the following parameters:

- o refractive index of the substance between the prisms,
- o dispersion medium,
- o and their dependence on temperature.

6   Photonic crystals properties

The following lecture is based on MIT lectures about photonic crystals (Joannopoulos, 2008; Steven G. Johnson and J. D. Joannopoulos, 2003).

The main objective of photonics is the confinement of light in one or more directions for as long as possible. An objective for the next few years is currently defined as the creation of small, compact devices capable of optical signal processing using low powers – integrated optoelectronics. Photonic crystals have all the features that make them candidates for solving problems that will occur along the way towards reaching the objective defined above. The desired device is sometimes called optical transistor. In three figures that follow, Fig. 6.1, Fig. 6.2, Fig. 6.3, different types of photonic crystals are schematically depicted..
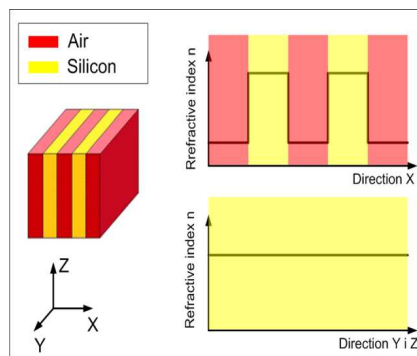
Fig. 6.1 Idea of 1D photonic crystal (1D PhC). Refractive index distributions along the x-, y-, and
z-direction.
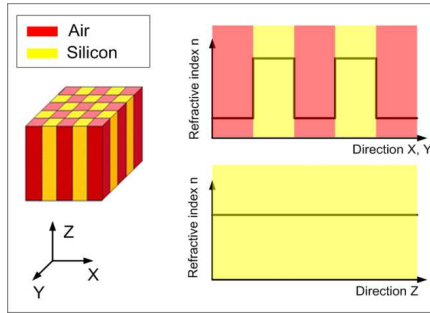
Fig. 6.2 Idea of 2D photonic crystal (2D PhC). Refractive index distributions along the x-, y-, and z-direction.
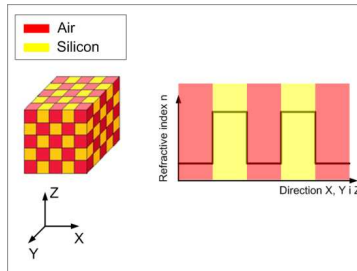
Fig. 6.3 Idea of 3D photonic crystal (3D PhC). Refractive index distribution along the x-, y-, and z-direction.

6.1 Mathematical description

What do we need to understand PhC theory? The following tools are essential:

- linear algebra
- Maxwell's equations
- Bloch theorem
- crystallography
- numerical analysis (e.g. FDTD)

$$\vec{E}, \vec{H} \sim e^{i(\vec{k} \cdot \vec{x} - \omega t)}$$

$$\left| \vec{k} \right| = \omega / c = 2\pi / \lambda$$
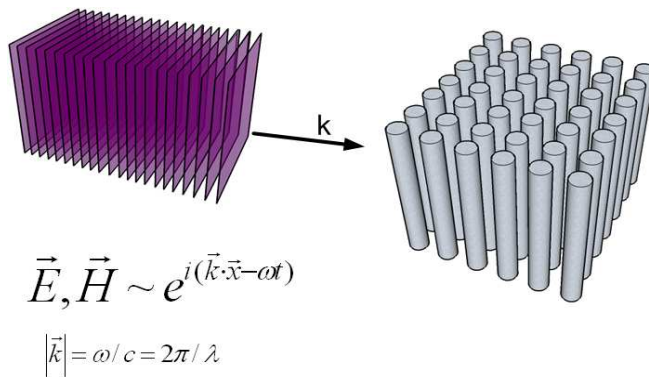
Fig. 6.4 Plane wave characterized by a wave vector *k* in a 2D PhC.

54

In figure Fig. 6.4 an example of a 2D PhC is presented together with a schematical view an electromagnetic plane wave. A characteristic feature of PhCs is their ability to guide (pass) electromagnetic plane waves without scattering for some selected (crystal construction-dependent) values of wavelength λ. However, it is always the case that for wavelengths $\lambda \sim 2a$, light (or, in general, electromagnetic wave from any other frequency range) cannot propagate in PhC. Here, a is the lattice constant of the crystal. In fact, similar phenomenon occurs when propagation of electrons through crystal structure materials (or crystals; not to be confused with photonic crystals) is considered. When electron propagation takes place in amorphous materials (materials without crystal structure) (see figure Fig. 6.5) electronic conductivity is significantly worse than that in crystal structure materials like e.g. copper (see figure Fig. 6.6). Such a notable difference in conductivity values is a result of electrons being actually waves rather than point-like particles. According to Schrödinger equation, in periodic media, waves can propagate without scattering. Solution of Schrödinger equation for a single period of medium periodicity is called Bloch theorem.
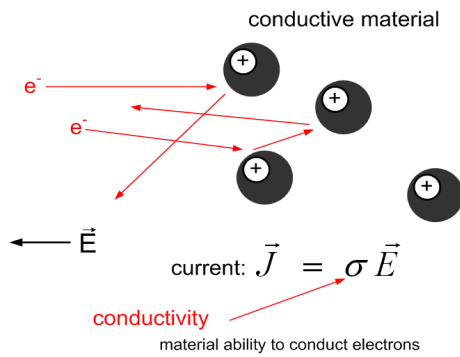
Fig. 6.5 Electronic conductivity in amorphous materials.
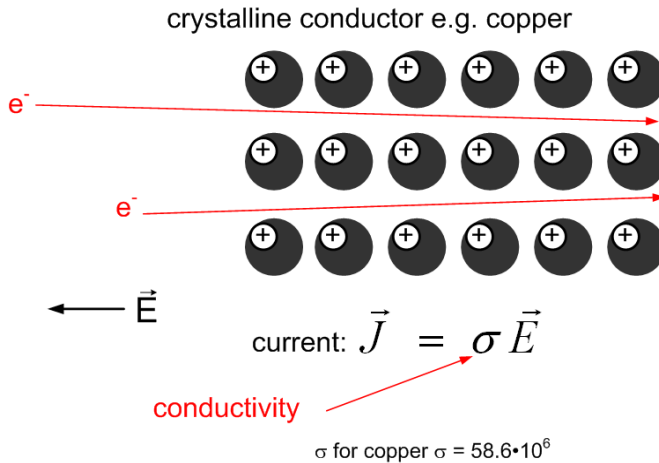
Fig. 6.6 Electronic conductivity in crystal structure materials.

Since electrons as well as photons show wave-like behavior, there must be some degree of similarity of the mathematical description of how the above particles move through periodic

media. In figure Fig. 6.7, a very instructive comparison between electronics and optics is presented.

atoms in silicon crystal

array of dielectrics pillars

periodic medium

band diagram (dispersion relation)

electrical band gap

photonic band gap

frequency

frequency

wavevector k

wavevector k
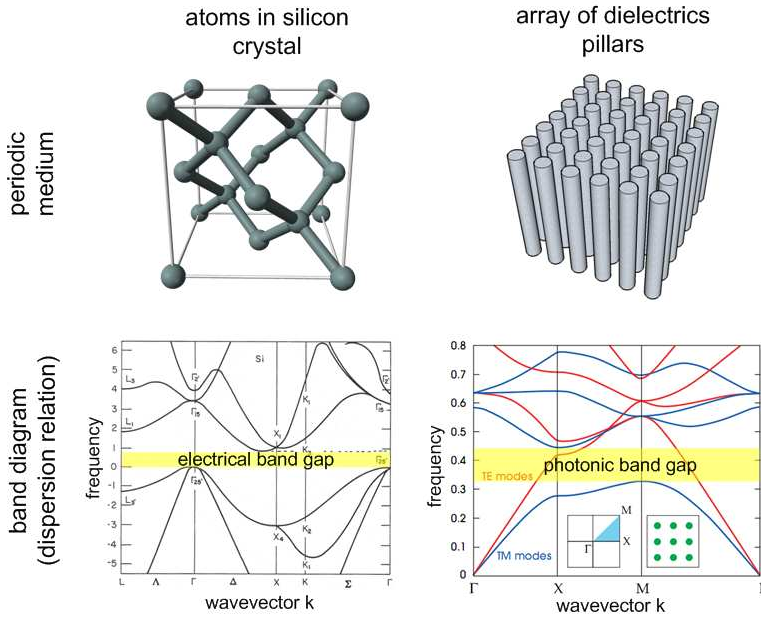
Fig. 6.7 Analogies between the propagation of electrons in silicon and the propagation of light in a 2D PhC.

For the description of light propagation in photonic crystals, main equation of photonic crystal analysis is used. It is derived from Maxwell's equation and has the form

$$\vec{\nabla} \times \left(\frac{1}{\varepsilon(\vec{r})} \vec{\nabla} \times \vec{H}(\vec{r}) \right) = \left(\frac{\omega}{c} \right)^2 \vec{H}(\vec{r}) \tag{6.1}$$

In order to find propagated plane waves in photonic crystal, solving the base equation for specific structure $\varepsilon(x,y,z)$ is needed. At the end of math work, distribution of vector magnetic field will be found $H(x,y,z)$ for specific frequency of the electromagnetic wave. Electrical field $E(x,y,z)$ can then be found by solving one of Maxwell's equations given below

$$\vec{E}(\vec{r}) = \left(\frac{-ic}{\omega\varepsilon(\vec{r})} \right) \vec{\nabla} \times \vec{H}(\vec{r}) \tag{6.2}$$

If the product of a matrix and a vector equals (is supposed to equal) the product of a scalar and this vector, we deal with the so called eigenvalue problem. The eigenvalue problem can be written in form of an equation

$$A \cdot v = \lambda \cdot v \tag{6.3}$$

The base equation (6.1) is an example of an eigenvalue problem.

In more technical terms, by comparing (6.1) and (6.3), we can see that $H(r)$ plays a role of the eigenvector (v), the expression $(\omega/c)^2$ is the eigenvalue (λ), and the operator (operators) acting on $H(r)$ in the left-hand side of (6.1), plays the role of the matrix (A) from (6.3).

56

6.2   Scale invariance of Maxwell equations

Maxwell's equations are scale-invariant thus base equation is independent of any chosen values of structure sizes and wavelength. Let us assume a medium of constant distribution of permittivity $\varepsilon(r)$ and the magnetic field $H(r)$ of the frequency ω. Now, we would like to find the magnetic filed distribution in some different medium $\varepsilon'(r)$, which is a rescaled (i.e. compressed or extended) version of $\varepsilon(r)$. A rescaling factor is s

$$\varepsilon(r): \varepsilon'(r) = \varepsilon(^r/_s) \tag{6.4}$$

$$\vec{r}' = \vec{r} \cdot s \tag{6.5}$$

$$\vec{\nabla}' = \vec{\nabla}/s \tag{6.6}$$

Applying the base equation (6.1), we find the magnetic field and the frequency for the rescaled medium

$$\vec{\nabla} \times \left(\frac{1}{\varepsilon(\vec{r})} \vec{\nabla} \times \vec{H}(\vec{r}) \right) = \left(\frac{\omega}{c} \right)^2 \vec{H}(\vec{r}) \tag{6.7}$$

On inserting (6.5) and (6.6) into (6.7), we get

$$s\vec{\nabla'} \times \left(\frac{1}{\varepsilon(\vec{r'}/s)} s\vec{\nabla'} \times \vec{H}(\vec{r'}/s) \right) = \left(\frac{\omega}{c} \right)^2 \vec{H}(\vec{r'}/s) \tag{6.8}$$

After straightforward rearrangements, we arrive at the following equation

$$\vec{\nabla'} \times \left(\frac{1}{\varepsilon'(\vec{r'})} \vec{\nabla'} \times \vec{H}(\vec{r'}/s) \right) = \left(\frac{\omega}{sc} \right)^2 \vec{H}(\vec{r'}/s) \tag{6.9}$$

Sense of the equation (6.9) is usually stated in general terms as follows: the magnetic filed and mode frequency in scaled medium equal the magnetic filed and frequency in original medium divided by a scaling factor s. It is also expressed bellow

$$\vec{H'}(\vec{r}') = \vec{H}(\vec{r'}/_s) \tag{6.10}$$

$$\omega' = \omega/s \tag{6.11}$$
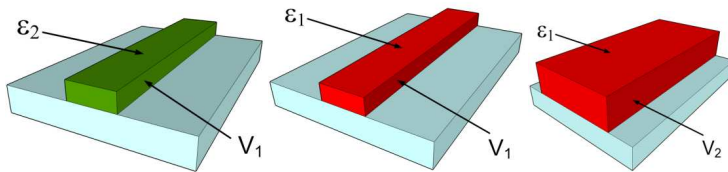
Fig. 6.8 Three systems in which either geometry or dielectric constant value has been rescaled.

Figure shows an example of three physical systems in which either geometrical parameters (system's dimensions) or material parameters (dielectric constant value) have been rescaled. Solution of Maxwell's equations for one system determines the solution for any other system derived from the base system by means of rescaling it.

6.3 Periodicity

Photonic crystal is a periodic structure (see figure Fig. 6.9), which can be analyzed with the equation (6.1) (base equation) by assuming a periodic distribution of dielectric constant

$$\varepsilon(\vec{r}) = \varepsilon(\vec{r} + \vec{R}) \tag{6.12}$$
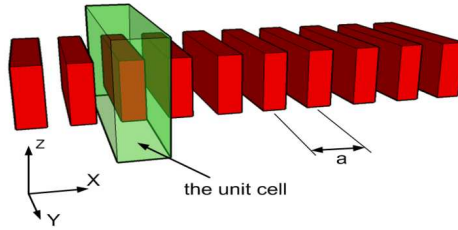
Fig. 6.9 Regular configuration of dielectric blocks – an example of a simple photonic crystal.

If propagation medium is periodic, it is not necessary to analyze the entire medium. Instead, due to medium periodicity, it is enough to consider only a single unit cell of the medium. Due to mathematical reasons, a convenient tool in this regard is the so called reciprocal lattice, the idea of which is shown in figure Fig. 6.10.
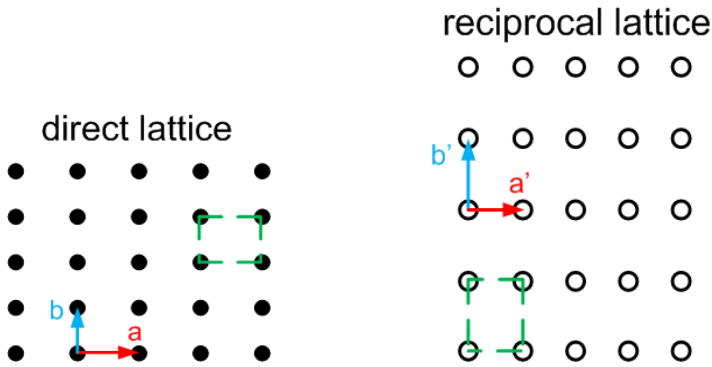
Fig. 6.10 Relationship between the real and reciprocal lattices.

Reciprocal lattice is (mathematically) created according to equations given below

$$\vec{a}' = 2\pi \frac{\vec{b} \times \vec{c}}{\vec{a}(\vec{b} \times \vec{c})} \tag{6.13}$$

$$\vec{b}' = 2\pi \frac{\vec{c} \times \vec{a}}{\vec{a}(\vec{b} \times \vec{c})} \tag{6.14}$$

$$\vec{c}' = 2\pi \frac{\vec{a} \times \vec{b}}{\vec{a}(\vec{b} \times \vec{c})} \tag{6.15}$$

$$\vec{a}' \times \vec{a} = 1 \tag{6.16}$$

$$\vec{b}' \times b = 1 \tag{6.17}$$

Photonic crystal band diagrams show Bloch modes of irreducible Brillouin zone, which is an area (or volume in 3D case) reduced according to Brillouin zone symmetry.
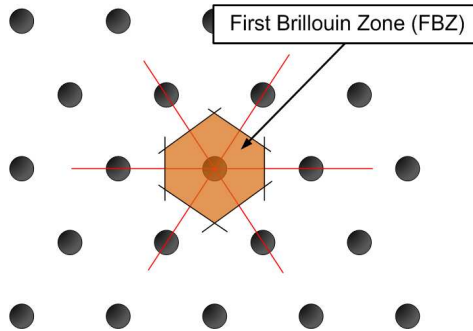
Fig. 6.11 Method of determining the first Brillouin zone.

In figure Fig. 6.12, two common types of photonic crystal lattice are shown: regular lattice (on the left) and triangular lattice (on the right). Also irreducible Brillouin zones are shown for which band diagrams are calculated.
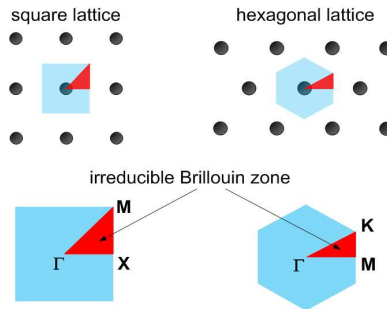
Fig. 6.12 Examples of irreducible Brillouin zones of two of the symmetry types possible in 2D PhCs.

When permittivity is a periodic function, solution of base equation takes the form

$$\vec{H}(\vec{r}) = e^{i\vec{k}\vec{r}} H_{n,\vec{k}}(\vec{r}) \tag{6.18}$$

Eigenvalue of the above equation takes the form of a discrete function of frequency depending on wavevector

$$\omega_n(k) \tag{6.19}$$

If analyzed structure is periodic in any direction, that means unit cell has finite volume, eigenvalue $\omega_n(k)$ (optical angular frequency in the function of propagation constant) is a discrete function with n = 1,2,3 …. Group of eigenvalues $\omega_n(k)$ calculated for consecutive values of k constitutes a group of (continuous) functions called band diagram
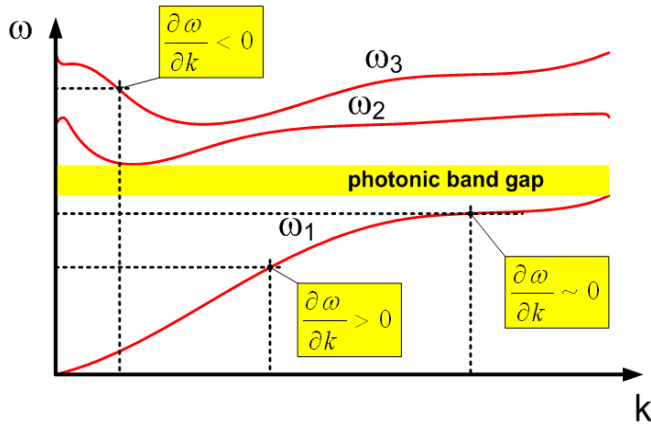
Fig. 6.13 Band diagram of a PhC – sample data.

Solving the base equation for periodic structure is not an easy task. Suitable numerical methods of analysis are crucial. There are three groups of numerical methods utilized in photonics:

- ○ **time domain** – solver of real 3D structure with boundary condition by give time,
- ○ **transmission matrix** – analyzed mode is divides into smaller cells or layers; for each layer, transmission or reflection matrix is found; finally, all the transmission or reflection matrices are used to find transmission and reflection coefficients of entire structure,
- ○ **frequency domain** – direct Bloch mode solver.

6.4   Why 2D photonic crystals

- ○ 1D PhCs – their parameters strongly depend on incidence angle of light.
- ○ 3D PhCs – able to provide complete photonic bandgaps, however, sophisticated technologies are required to fabricate them; they also exist in nature.
- ○ **2D PhCs are a compromise** – the well-know planar technology; photonic crystal features are observed only in two dimensions and usually, to confine light in the third direction, total internal reflection (TIR) is used (see figure Fig. 6.14).
- ○ **2.5D** – the same as 2D, but instead of TIR, multilayer structures are used as additional 1D photonic crystals extending in the third direction.
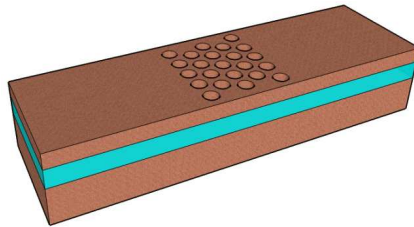
Fig. 6.14 2D PhC etched in a planar waveguide structure.

6.5   Devices

Photonic crystals are able to confine the optical mode in a small volume *V* for a long time τ. In formula below, the factor *F* provides (an indirect) information on how long the electromagnetic field stays confined within cavity.

$$F = \frac{\tau}{T} \times \frac{\lambda^3}{V}$$ (6.20)

$$Q = \frac{2\pi\tau}{T}$$ (6.21)

Meanings of the symbols are: λ – wavelength in vacuum, T – oscillation period, and Q – quality of cavity.

Many kinds of photonic devices work by utilizing the third-direction light confinement based of total internal reflection.
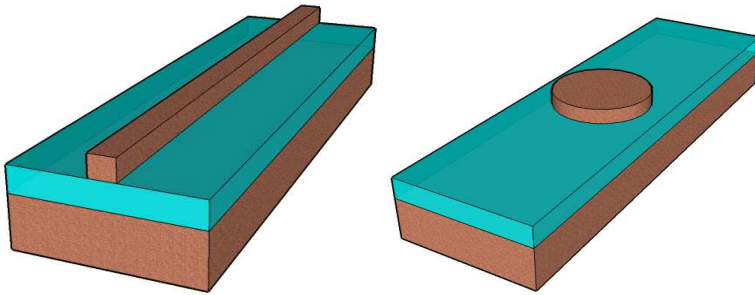
Fig. 6.15 Strip waveguide (left) and microdisc (right) – examples of utilizing total internal reflection to provide light confinement in the third (vertical) direction.

There are also PhC-based devices that work utilizing photonic bandgap or other phenomena instead of total internal reflection for confining light in the third direction. Photonic crystal-based devices can work in several different modes, e.g.:

- **PBG** – photonic bandgap in one, two or three directions,
- **PBE** – photonic band edge – point where group velocity of propagated light slows down to nearly zero – „slow light" .

In the modes mentioned above, photonic crystal-based device, as it is commonly said, operates below light line or above light line. The first case is realized when TIR condition is fulfilled. The second condition is realized otherwise, i.e. when TIR condition is not fulfilled.

Tab. 1.1. Examples of PhC-based photonic devices.

	Below light line	**Above light line**
PBG	o micro-cavity (QED) o micro-lasers o waveguides o "add-drop" filter o ...	o "drop" filter o ...

| PBE | o direction "drop" filter
o micro-lasers
o superprism
o devices for pulse regeneration
o ... | o micro-mirrors
o all-optical switches
o micro surface lasers
o ... |

7 Photonic crystals technology

In order to fabricate a PhC-based device, like e.g. a mirror shown in figure Fig. 7.1, we can choose one of several methods. The method of choice often depends on the material in which PhC structure is supposed to be created. In figure Fig. 7.2, two broad categories of technological methods are schematically depicted. Photonic structures can be fabricated going "from bottom to top" (up) or "from top to bottom" (down).
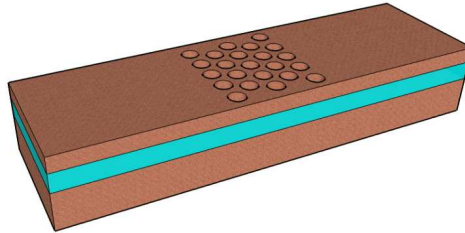
Fig. 7.1 Planar mirror employing a PhC.

In methods belonging to the first category, photonic crystal structure "grows" on a substrate. Example technologies realizing this kind of fabrication are: structure growth by means of a mask or by means of self-organization. In the first case, substrate material is (partially) removed. For this, dry etching methods are usually used in practice. For 2D PhCs fabricated in planar structures, methods belonging to the "from top to bottom" category are used most often.
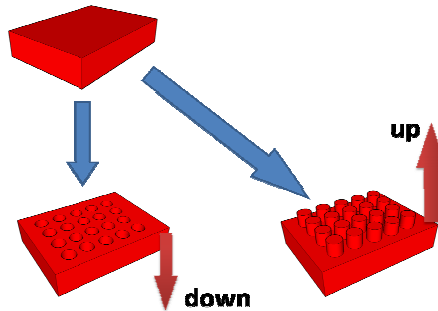
Fig. 7.2 Two broad categories of planar PhC fabrication methods.

7.1 Lithography

Usually, the first technological step is the design of a lithographic mask. The mask will later be used for transferring the photonic structure pattern (geometry) onto material surface. Choosing a mask is based on the lithographic method that is intended to be used. Currently, four most commonly used lithographic methods can be listed:

- o electron beam lithography – serial method; beam of electrons writes pattern line by line
- o lithography DUV – deep UV 248 nm 193 nm – lithography known from the CMOS technology
- o imprinting – parallel method; utilizes master stamp (master) to mold patterns in resist
- o interference lithography – parallel method; utilizes two laser beams that interfere on sample surface

7.1.1 Electron beam lithography

An idea of electron lithography (electron beam lithography) is shown in figure Fig. 7.3. First, structure's mask is designed by using specialized software (see figure Fig. 7.4 for an example). Based on the mask, electron beam is directed so that it draws (writes) the structure pattern line by line.
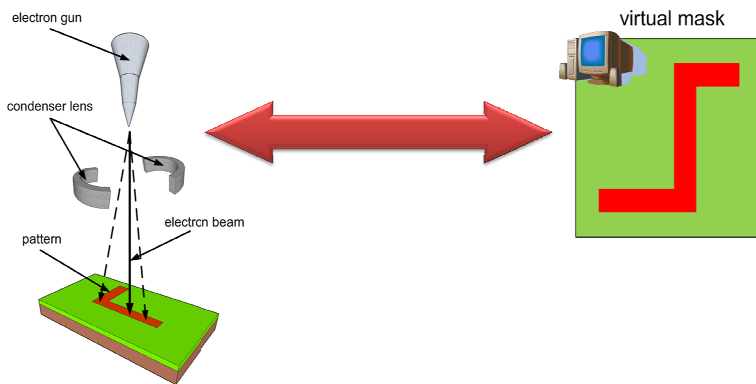
Fig. 7.3 Idea of electron lithography (electron beam lithography).

A significant advantage of this method is its high resolution, down to <100nm. The resolution depends on the kind of photoresist and on the energy of electrons. A disadvantage is a relatively small writing area. Writing in several areas positioned side by side leads to so called stitching errors. In photonic crystals, where precision of positioning of each crystal feature (e.g. hole) is critical, stitching errors need to be maintained at very low levels. Due to serial-type operation, thus being very time consuming, electron lithography is mainly used in academic research.
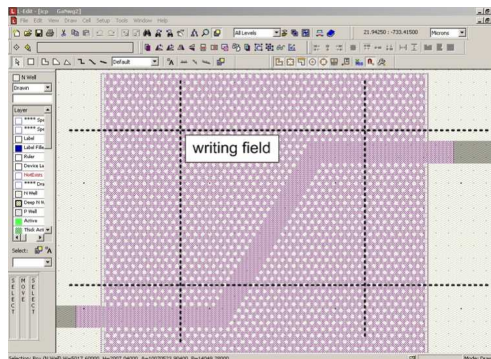
Fig. 7.4 Screenshot of a software application enabling the lithography mask design.

7.1.2 Lithography DUV

One of lithographic techniques of commercial importance, is the Deep UV (DUV) lithography shown in figure Fig. 7.5. It is analogous to a traditional lithography known from the CMOS technology. However, because of different sizes of structure details, different light wavelengths are used.
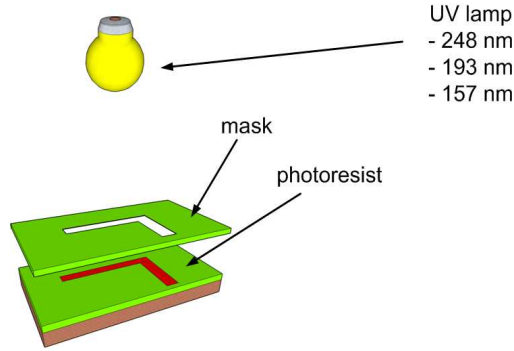
Fig. 7.5 Lithography employing the deep UV radiation.

A significant advantage of the method is the parallel mode of operation. Method's resolution depends on the light wavelength in use – the shorter the wavelength, the better the resolution. Designing a mask (mechanical mask) is an important step of the entire process. Diffraction effects at mask corners need to be taken into consideration and appropriately compensated by means of including special compensating patterns. As a result, obtaining a precision photonic pattern proves challenging.

7.1.3 Nano-imprinting

Another parallel-mode method is nano-imprinting. It is widely used in industry. An appropriately shaped master stamp (master) is imprinted in a polymer layer as illustrated in figure Fig. 7.6. Then, after polymer hardening by means of UV-light, the mask is ready.
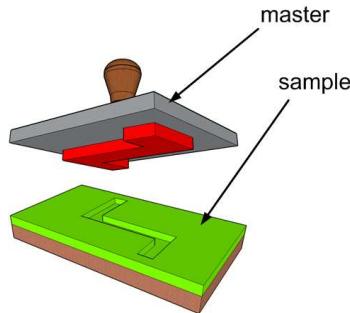
Fig. 7.6 Example of lithography based on imprinting.

During a single process, mask of virtually any size can be created. Pattern precision is mainly limited by stamp quality. Method's major advantage is its simplicity, thus cost efficiency. Unfortunately, a residual layer of photoresist that remains (in structure pattern) after imprinting needs to be removed with an additional technological process. Usually, a short-time oxygen plasma etching is applied.

7.1.4 Roll-to-roll imprinting

The most popular among commercial imprinting methods is the roll-to-roll imprinting. Consecutive process steps are performed in a continuous manner by means of rollers. Each roller imprints a different pattern (different part of the entire pattern). In figure Fig. 7.7, part of technological line is shown. This part (one roller) only imprints a single fragment of the entire pattern.
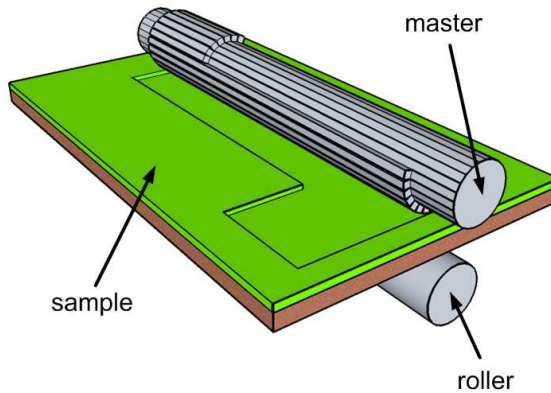
Fig. 7.7 Lithography based on roll-to-roll imprinting.

7.1.5 Interference lithography

A relatively simple lithographic method especially well suited for large areas, is the interference lithography. Laser beam is split into to beams and, by using an appropriate optical setup, they are directed at the sample. The beams then interfere on sample surface and photoresist layer present on the sample surface is exposed to a series of alternating bright and dark lines (interference fringes).
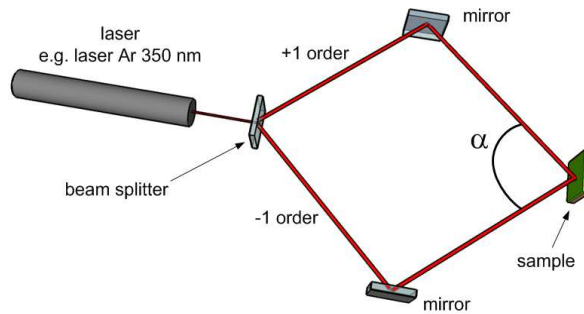
Fig. 7.8 Experimental interference lithography setup.

By using an optical beam expander, writing large-area patterns is possible. A significant advantage offered by the process lies in that it avoids using masks. Periodic patterns are created in a single technological step. By changing angle α, spatial period of patterns can be adjusted according to the equation

$$\Lambda = \frac{\lambda/2}{\sin\left(\alpha/2\right)} \tag{7.1}$$

Photoresist exposure depth and periodicity filling factor are affected by optical power of the interfering beams. Due to the interferometric nature of the process, sinusoidally shaped patterns are written in photoresist as shown in figure Fig. 7.9.
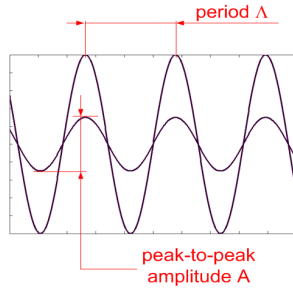
Fig. 7.9 Influence of laser (light source) power on the depth of patterns written in photoresist.

Figure Fig. 7.10 shows, how 2D patterns can be produced by means of rotating the sample by angle Θ. In figure Fig. 7.11, several patterns are shown that are possible to be written with interferometric lithography.
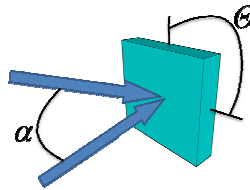
Fig. 7.10 Idea of multiple exposition employed in interference lithography for the creation of 2D patterns .
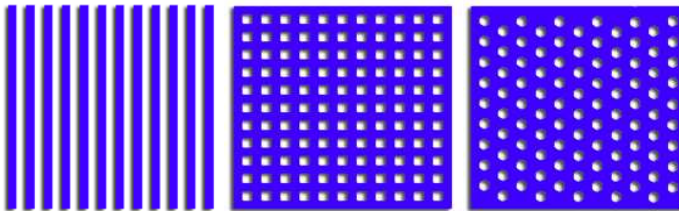
Fig. 7.11 Examples of patterns that can be written with interference lithography. Numbers of expositions used are (from left to right): 1, 2, and 3. In the last two cases, rotation by angle Θ = 90° or Θ = 60°, respectively, needs to be used.

In figure Fig. 7.12, photograph of a laboratory setup enabling the interference lithography is presented. All setup elements are named.
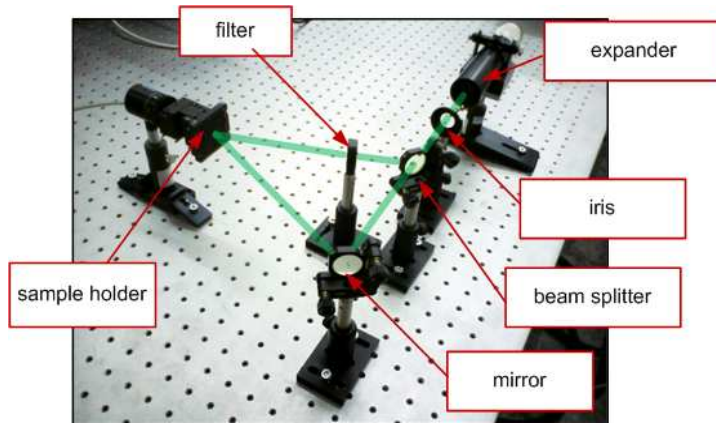
Fig. 7.12 Photograph of an interferometric lithography laboratory setup.

Microscopic images of 2D periodic patterns written in photoresist by means of interference lithography are presented in figures Fig. 7.13 and Fig. 7.14. Images in the first figure come from an optical microscope. Image in the second figure was obtained with an AFM microscope.
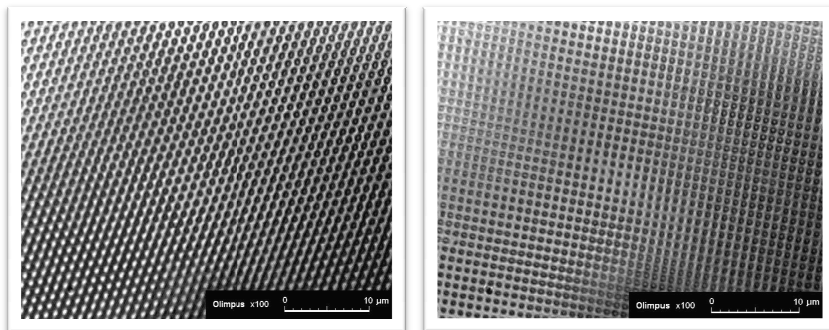
Fig. 7.13 Optical microscope images of 2D periodic patterns produced in photoresist by means of interference lithography.
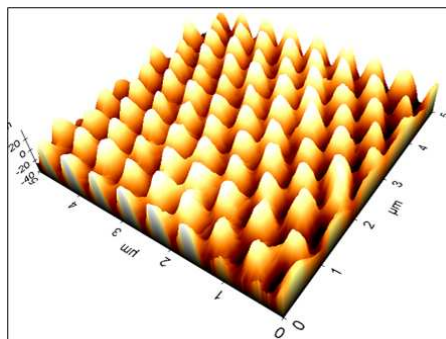
Fig. 7.14 AFM microscope image of a 2D periodic pattern produced in photoresist by means of interference lithography.

7.2 Dry etching

After desired pattern has been written in a photoresist layer by using any of the methods discussed in previous paragraphs, the pattern is about to be transferred into the target material, e.g. optical planar waveguide. Due to the "from top to bottom" approach we have chosen, we will now focus our attention on methods that allow the target material to be removed (at places defined by openings in photoresist). Such methods are called etching and they fall into two broad categories: wet etching, conducted in liquid chemical solutions, and dry etching, conducted with plasma or heavy ions. Due to low dimensions (dimensions of smallest details that need to be etched) of photonic structures, employing wet etching methods is usually not possible. Thus, below only dry etching methods will be discussed.

Every etching process can be characterized by the following parameters:

- etching selectivity (see formula (7.2)) – ratio of target material etching speed V_w to mask etching speed V_r
- etching speed
- anisotropy – indirectly expressed as slope of etched pattern sidewalls

$$S = \frac{V_w}{V_r} \tag{7.2}$$

Dry etching utilizes gas plasma in order to remove molecules and atoms from substrate (target material). Dry etching can be divided into three groups according to etching mechanism:

- chemical process – chemical reaction between plasma gases and substrate remove material from substrate
- physical process – ion bombardment removes substrate material
- combination both chemical and physical processes

Photonic applications usually need more sophisticated methods of etching than that needed in electronic applications. It is because photonic structures usually require higher anisotropy and larger etching depth in order to function as designed. Due to these reasons, etching process is often conducted in two steps. So called intermediate mask is used. First, pattern written in photoresist is transferred to a thin layer of e.g. SiO_2 earlier evaporated on the target material. After etching and hardening processes, the SiO_2 layer becomes the intermediate mask. Such an intermediate mask is much less prone to all kinds of damage and it ensures high etching selectivity. Thanks to these intermediate mask features, the second etching process can proceed for a longer time thus allowing deeper and low side-wall angle patterns to be produced in target material.

Reactive Ion Etching (RIE) / Inductive Coupled Plasma (ICP) – is a combination of chemical processes, which reduce chemical bonding strength between atoms of the substrate, and physical processes, which use heavy ions to release atoms from the substrate.

Physical etching is conducted by ion bombardment

- isotropic
- defects
- less selective

Chemical etching is conducted be chemical reaction between reactive plasma and substrate material

- anisotropic
- high selective
- quick

Figure Fig. 7.15 shows processes that occur during RIE/ICP etching. Heavy ions, by hitting the substrate, can either release substrate atoms or introduce substrate defects thus reducing

chemical bonding strengths between atoms and molecules. Reactive molecules can be absorbed and then desorbed.
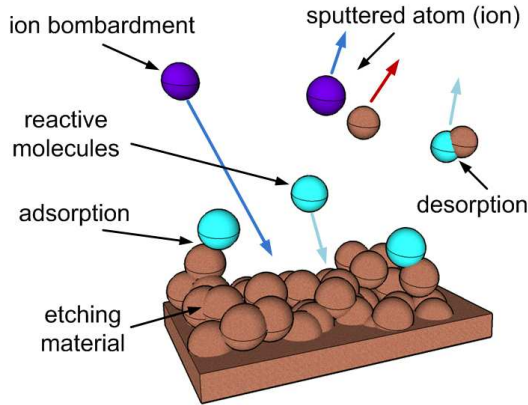
Fig. 7.15 Processes possible in RIE/ICP etching.

7.3 Focused Ion Beam etching

Focused Ion Beam (FIB) etching systems usually utilize Ga^+ ions for bombarding the sample surface. FIB etching systems are very similar to e-beam systems, where electrons are used for surface investigation (during the process, electrons being released from sample are gathered and thus sample surface image is created).

Typical parameter values of FIB process:

- o ion energy 10-50 keV
- o beam diameter < 30 nm
- o FWHM <30 nm @ 70 keV
- o Gaussian beam

Examples of 300 nm diameter holes etched with FIB process are presented in figure Fig. 7.16.
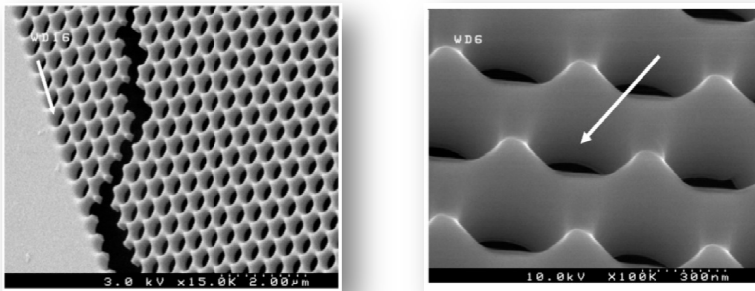
Fig. 7.16 SEM microscope images (SEM micrographs) of periodic patterns produced by means of FIB etching (Freeman, Madden, & Luther-Davies, 2005)**.**

7.4 Measurements

After a photonic device has been designed and manufactured, device characterization is usually performed. Depending on which of the device parameters are most important to us, or in which operation mode the device will work (i.e. transmission, reflection) several measurement (characterization) method types can be used. The method types are schematically depicted in figure Fig. 7.17. Transmission / reflection methods and methods based on coupling light into waveguide are shown.

Common parameters:

- o transmission, $T(w)$
- o reflection, $R(w)$
- o diffraction, $D(w)$
- o absorption, $A(w)$
- o losses, $L(w) = 1\text{-}T\text{-}R\text{-}D\text{-}A$
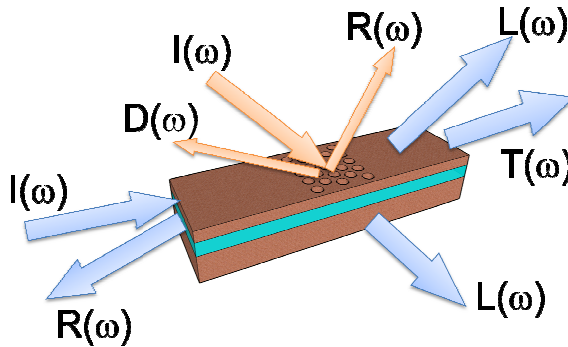
Fig. 7.17 Optical signals available for measuring during characterization of photonic structures.

Another classification considers the measurement light source location:

- o external source of light
    - o reflection methods
    - o end-fire method
- o internal source of light
    - o transmission method with internal source
    - o luminescence method

7.4.1   End-fire method

A popular, although not very simple, measurement method is end-fire coupling. In figure Fig. 7.18, schematic view of a measurement setup is shown. A sample is placed on a table. Table position can be adjusted in three directions with a submicrometer accuracy. Optical signal is coupled into the sample with a fiber of a specially prepared end (see figure Fig. 7.19), which focuses light on the sample edge. Output signal is collected by a microscope objective and directed onto a photodetector.

70
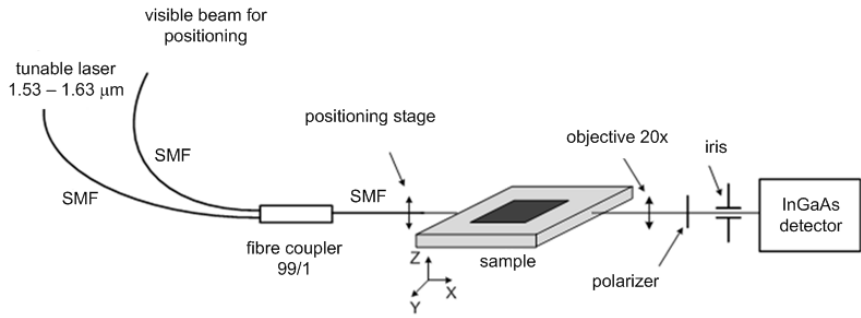
Fig. 7.18 Schematic view of a measurement setup in which end-fire coupling is utilized.
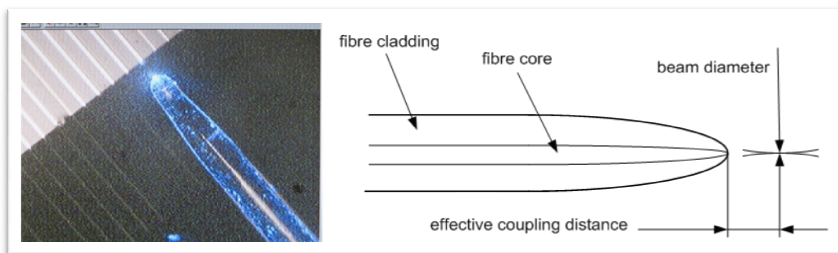
Fig. 7.19 Photography and drawing of an optical fiber prepared in a way suitable for end-fire coupling.
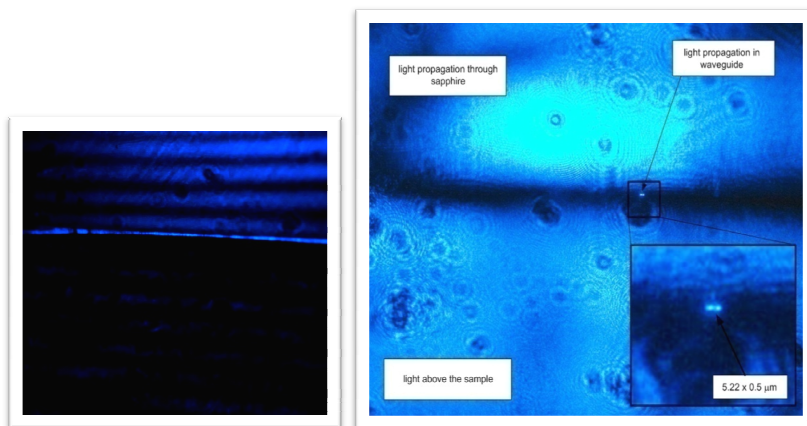
Fig. 7.20 Example images registered after light has been coupled into a planar waveguide (left) and a strip waveguide (right).
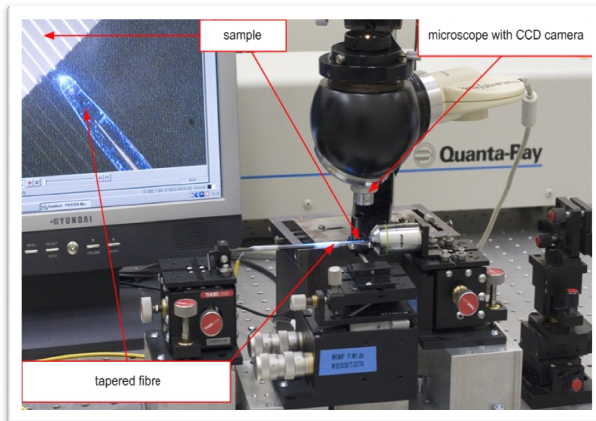
Fig. 7.21 Photograph of end-fire coupling laboratory setup – positioning elements.
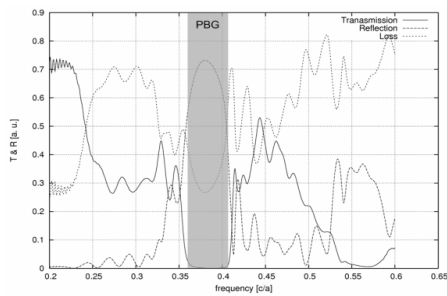
Fig. 7.22 Example transmission results for 2D PhCs.

Sample measurement results obtained with end-fire coupling applied to a 2D PhC are shown in figure Fig. 7.22. Photonic bandgap is marked in grey.

7.4.2 Reflection method

In the reflection method, configuration shown in figure Fig. 7.23 is applied. Sample is illuminated from top and either the reflected on transmitted signal is measured.

Measurement types:

- o   intensity of light for various angles of incidence at a fixed wavelength
- o   intensity of light for various wavelengths at a fixed angle of incidence
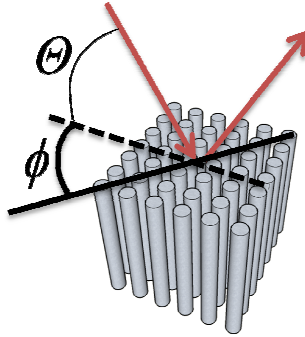
Fig. 7.23 Idea of reflection method. Light incidence angle is denoted as Θ.

In the method discussed, the reflected light carries information about PhC's band diagram (see figure Fig. 7.24) and about shape of PhC's periodic pattern. Peaks visible in reflection spectrum at different angles of incidence, appear for Bloch modes and when considered together they compose PhC band diagram.
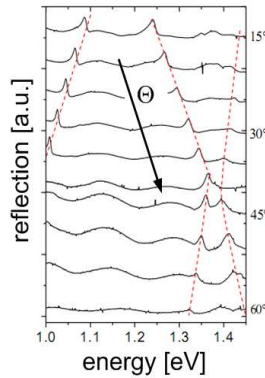
Fig. 7.24 Determining the PhC band diagram (red lines) by means of multiple reflection-spectra (A. D. Bristow, 2003)**.**

7.4.3 Internal source

Instead of coupling light that comes from an external source, there is a possibility of creating a light source combined with a photonic device already at the stage of device manufacturing. Example of light source type and of its location is shown in figure Fig. 7.25. Internal source-based solutions enable a significant simplification of device characterization process. Nevertheless, it is not always possible to integrate light source and photonic device during manufacture. In cases when integration is possible, quantum wells or rare-earth doping are used.

quantum wells – integrated
source of light

output
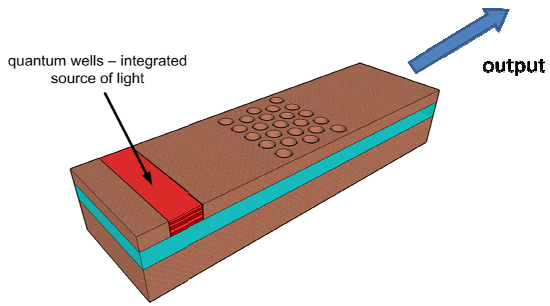
Fig. 7.25 Measurements performed with light source integrated with photonic device during manufacture.

References

A. D. Bristow. (2003). Optical Investigation of AlGaAs Photonic Crystal Waveguides.

Akiyama, T., & Fujita, H. (1995). A Quantitative Analysis of Scratch Drive Actuator Using Buckling Motion. Micro Electro Mechanical Systems, 1995, MEMS '95, Proceedings. IEEE (pp. 324-329).

Aksyuk, V. A., Pardo, F., Bolle, C. A., Arney, S., Giles, C. R., & Bishop, D. J. (2000). Lucent Microstar Micromirror Array Technology for Large Optical Crossconnects. Proc. SPIE 4178 (pp. 320-324).

Aoyagi, T., Aoyagi, Y., & Namba, S. (1976). High-efficiency blazed grating couplers. Applied Physics Letters, 29(5), 303. $abstract.copyright_name.value. Retrieved February 2, 2011, from http://link.aip.org/link/APPLAB/v29/i5/p303/s1/html.

Beer-Lambert Law. (2010). Wikipedia. Retrieved from http://en.wikipedia.org/wiki/Beer–Lambert_law.

Dylewicz, R. R. (2007). Fabrication, measurements and modelling of grating couplers integrated with gallium nitride planar waveguides.

Ellipsometry Tutorial. (2010). . Retrieved 2010, from http://www.jawoollam.com/tutorial_2.html.

Form Talysurf Brochure. (2010). .

Franken, P. A., Hill, A. E., Peters, C. W., & Weinreich, G. (1961). Generation of Optical Harmonics. Phys. Rev. Lett., 7(4), 118–119.

Freeman, D., Madden, S., & Luther-Davies, B. (2005). Fabrication of planar photonic crystals in a chalcogenide glass using a focused ion beam. Optics Express, 13(8), 3079. OSA. Retrieved February 1, 2011, from http://www.opticsexpress.org/abstract.cfm?URI=oe-13-8-3079.

Gill, D. S. (1996). Fabrication and characterisation of thin film optical waveguides by pulsed laser deposition.

Harper, K. R. (2003). Theory, design, and fabrication of diffractive grating coupler for slab waveguide.

Hecht, E., & Zajac, A. (1997). Optics (p. 694). Addison Wesley Publishing Company. Retrieved February 2, 2011, from http://www.amazon.com/Optics-Eugene-Hecht/dp/0201838877.

Joannopoulos, J. D. (2008). Photonic crystals: molding the flow of light (p. 286). Princeton University Press. Retrieved January 31, 2011, from http://books.google.com/books?id=owhE36qiTP8C&pgis=1.

Kogelnik, H. (1969). Coupled wave theory for thick hologram gratings. The Bell System Technical Journal, 48(9), 2909-2947. Retrieved from http://adsabs.harvard.edu/abs/1969BSTJ...48.2909K.

Kurzak, K. (2010). Spektroskopowe metody analityczne. Opole.

Lin, L. Y., Goldstein, E. L., & Tkach, R. W. (1999). Free-Space Micromachined Optical Switches for Optical Networking. IEEE Journal of Selected Topics in Quantum Electronics, 5(1), 4-9.

Lin, L. Y., Goldstein, E. L., & Lunardi, L. M. (2000). Integrated signal monitoring and connection verification in MEMS optical crossconnects. IEEE Photon. Technol. Letters, 12(7), 885 - 887.

Liu, J.-ming. (2005). Photonic Devices (p. 1104). Cambridge University Press.

Ogawa, K., Chang, W., Sopori, B., & Rosenbaum, F. (1973). A theoretical analysis of etched grating couplers for integrated optics. IEEE Journal of Quantum Electronics, 9(1), 29-42. Retrieved February 2, 2011, from http://adsabs.harvard.edu/abs/1973IJQE....9...29O.

Palais, J. C. (1998). Fiber optic communications. Prentice-Hall.

Rebilas, K. (2010). Refraktometr Abbego. Pomiar współczynnika załamania i wyznaczanie stężenia roztworów. Cracow.

Stegeman, G. I. (1993). Material figures of merit and implications to all-optical waveguide switching. Proceedings SPIE Vol. 1852 (pp. 75-89).

Steven G. Johnson and J. D. Joannopoulos. (2003). Introduction to Photonic Crystals: Bloch's Theorem, Band Diagrams, and Gaps (But No Defects).

Szroeder, P. (2010). Rezonanse magnetyczne oraz wybrane techniki pomiarowe fizyki ciała stałego.

Tompkins, H. G., & Irene, E. A. (2005). Handbook of ellipsometry (p. 870). William Andrew. Retrieved February 2, 2011, from http://books.google.com/books?id=aLnm8bCOqJwC&pgis=1.

Ulrich, R. (1971). Optimum Excitation of Optical Surface Waves. Journal of the Optical Society of America, 61(11), 1467. Retrieved from http://www.opticsinfobase.org/abstract.cfm?URI=josa-61-11-1467.

Yeow, T.-W., Law, K. L. E., & Goldenberg, A. (2001). MEMS optical switches. IEEE Communications Magazine, 39(11), 158 - 163.

Ziętek, B. (2005). Optoelektronika (2nd ed., p. 615). Wydawnictwo Uniwersytetu Mikołaja Kopernika.

Łowkis, R. (1997). Efekty modulacji światła w heterostrukturach GaAs/AlGaAs.